NAVAL POSTGRADUATE SCHOOL

MONTEREY, CALIFORNIA

THESIS

EXPERIMENTS WITH THE REMUS AUV

by

Matthew D. Phaneuf

June 2004

Thesis Advisor: Anthony J. Healey

Approved for public release; distribution is unlimited

THIS PAGE INTENTIONALLY LEFT BLANK

REPORT DOCUMENTATION PAGE			Form Approved OMB No. 0704-0188

1. AGENCY USE ONLY *(Leave blank)*	2. REPORT DATE	3. REPORT TYPE AND DATES COVERED
	June 2004	Engineer's and Master's Thesis

4. TITLE AND SUBTITLE: Experiments with the REMUS AUV	5. FUNDING NUMBERS
6. AUTHOR(S) Matthew D. Phaneuf	
7. PERFORMING ORGANIZATION NAME(S) AND ADDRESS(ES) Naval Postgraduate School Monterey, CA 93943-5000	8. PERFORMING ORGANIZATION REPORT NUMBER
9. SPONSORING /MONITORING AGENCY NAME(S) AND ADDRESS(ES) N/A	10. SPONSORING/MONITORING AGENCY REPORT NUMBER

11. SUPPLEMENTARY NOTES The views expressed in this thesis are those of the author and do not reflect the official policy or position of the Department of Defense or the U.S. Government.

12a. DISTRIBUTION / AVAILABILITY STATEMENT	12b. DISTRIBUTION CODE
Approved for public release; distribution is unlimited	A

13. ABSTRACT (maximum 200 words)

This thesis centers around actual field operations and post-mission analysis of data acquired using a REMUS AUV operated by the Naval Postgraduate School Center for Autonomous Underwater Vehicle Research. It was one of many platforms that were utilized for data collection during AOSN II, (Autonomous Oceanographic Sampling Network II), an ONR sponsored exercise for dynamic oceanographic data taking and model based analysis using adaptive sampling. The vehicle's ability to collect oceanographic data consisting of conductivity, temperature, and salinity during this experiment is assessed and problem areas investigated. Of particular interest are the temperature and salinity profiles measured from long transect runs of 18 Km. length into the southern parts of Monterey Bay. Experimentation with the REMUS as a mine detection asset was also performed. The design and development of the mine hunting experiment is discussed as well as its results and their analysis. Of particular interest in this portion of the work is the issue relating to repeatability and precision of contact localization, obtained from vehicle position and sidescan sonar measurements.

14. SUBJECT TERMS	15. NUMBER OF PAGES
REMUS, AUV, autonomous underwater vehicle, mine hunting, AOSN	77
	16. PRICE CODE

17. SECURITY CLASSIFICATION OF REPORT	18. SECURITY CLASSIFICATION OF THIS PAGE	19. SECURITY CLASSIFICATION OF ABSTRACT	20. LIMITATION OF ABSTRACT
Unclassified	Unclassified	Unclassified	UL

NSN 7540-01-280-5500 Standard Form 298 (Rev. 2-89)
Prescribed by ANSI Std. 239-18

THIS PAGE INTENTIONALLY LEFT BLANK

Approved for public release; distribution is unlimited

EXPERIMENTS WITH THE REMUS AUV

Matthew D. Phaneuf
Lieutenant, United States Navy
B.S.M.E., University of South Carolina, 1997

Submitted in partial fulfillment of the
requirements for the degree of

MECHANICAL ENGINEER
and
MASTER OF SCIENCE IN MECHANICAL ENGINEERING

from the

NAVAL POSTGRADUATE SCHOOL
June 2004

Author: Matthew D. Phaneuf

Approved by: Anthony J. Healey
Thesis Advisor

Anthony J. Healey
Chairman, Department of Mechanical and Astronautical Engineering

THIS PAGE INTENTIONALLY LEFT BLANK

ABSTRACT

This thesis centers on actual field operations and post-mission analysis of data acquired using a REMUS AUV operated by the Naval Postgraduate School Center for Autonomous Underwater Vehicle Research. It was one of many platforms that were utilized for data collection during AOSN II, (Autonomous Oceanographic Sampling Network II), an ONR sponsored exercise for dynamic oceanographic data taking and model based analysis using adaptive sampling. The vehicle's ability to collect oceanographic data consisting of conductivity, temperature, and salinity during this experiment is assessed and problem areas investigated. Of particular interest are the temperature and salinity profiles measured from long transect runs of 18 Km. length into the southern parts of Monterey Bay. Experimentation with the REMUS as a mine detection asset was also performed. The design and development of the mine hunting experiment is discussed as well as its results and their analysis. Of particular interest in this portion of the work is the issue relating to repeatability and precision of contact localization, obtained from vehicle position and sidescan sonar measurements.

THIS PAGE INTENTIONALLY LEFT BLANK

TABLE OF CONTENTS

THIS PAGE INTENTIONALLY LEFT BLANK

LIST OF FIGURES

THIS PAGE INTENTIONALLY LEFT BLANK

LIST OF TABLES

THIS PAGE INTENTIONALLY LEFT BLANK

ACKNOWLEDGMENTS

First, I want to give thanks to Jesus Christ, my Lord and savior, who has given me so many opportunities and blessings. None of this would be possible without him.

I would like to thank my thesis advisor, Professor Anthony Healey. His guidance and instruction were invaluable. Not only did he teach me in the classroom and in the field but also through his example as a dedicated professional.

I am also grateful to Doug Horner, a research assistant for the NPS Center for AUV Research. He was extremely helpful and a great friend. I could not have finished without his assistance.

Finally, I would like to thank my family. To my wonderful wife, Leigh, I want you to know how much I appreciate the support and encouragement you always provide. To my children, Nick and Becca, I thank you for your patience and understanding when I could not always be there for you.

THIS PAGE INTENTIONALLY LEFT BLANK

I. INTRODUCTION

A. MOTIVATION

The importance of unmanned vehicles in military applications is unquestionable. The ability to deploy assets for reconnaissance and intelligence gathering into dangerous environments with no risk of human life is invaluable. Future utilization of these vehicles will no doubt reach levels of complexity and utility barely imaginable at the current state of the art.

The Chief of Naval Operations (CNO), Admiral Vern Clark, outlined his vision for the future of the Navy and its role in joint operations, Sea Power 21 (Clark, 2002). He detailed three concepts that the Navy needs for continued operational effectiveness. These are Sea Strike, Sea Shield, and Sea Basing. Unmanned vehicles are vitally important to these concepts as they directly contribute to knowledge dominance and situational awareness.

One type of unmanned vehicle, the Autonomous Underwater Vehicle (AUV), is rapidly growing in its utility for military operations. These vehicles have some substantial advantages over traditional unmanned underwater vehicles. They have onboard computers that store instructions necessary for performing tasks, their own power supply, and some degree of programmed autonomy. This autonomy is the ability to make decisions that are required to perform instructed tasks and, in some cases, to actually adjust their tasking based on the situation. The ability to make decisions greatly reduces the need for human intervention during an operation.

These characteristics allow AUVs to operate without a tether. Traditional UUVs need tethers to supply power and provide a link for control commands to and data transfer from the vehicle. The absence of a tether allows AUVs to perform operations far from the deploying vessel or port and enables travel through areas that would otherwise be prohibitive.

Autonomous Underwater Vehicles, AUVs, are a rapidly evolving technology. There are a myriad of different sizes, shapes, methods of propulsion, and sensor packages for the various AUVs in use today. These vehicles are utilized in an ever-expanding list of applications. In very general terms, though, AUVs are used for military, scientific, or commercial applications, with some overlap between them.

This thesis centers on actual field operation and post-mission analysis of data acquired using a REMUS AUV. REMUS, an acronym for Remote Environmental Measuring Units, is manufactured by Hydroid, Inc. and was originally developed at Woods Hole Oceanographic Institution. Its initial purpose was to be an oceanographic collection tool that was inexpensive, simple to use, and able to be deployed rapidly (von Alt, Allen, Austin, & Stokey 1994). It is currently utilized in a number of different applications, both military and oceanographic and is easily one of the most popular AUVs with over fifty units in use throughout the world (Jordan, 2003).

Mine detection is one military application in which REMUS and other AUVs have been utilized and will continue to find purpose. REMUS' small size and autonomy is especially valuable in the very shallow water region, 3 to 12 meters depth (von Alt, 2003), where searches by manned

submarines are impractical. This thesis documents experimentation that was designed to investigate the repeatability and precision of contact localization of REMUS mine detection results. Development, design, and results of this experimentation will be covered in Chapter II.

The REMUS operated by the Naval Postgraduate School Center for AUV Research was also one of many platforms utilized for data collection in the Office of Naval Research (ONR) sponsored AOSN II exercise. In this thesis, the vehicle's ability to collect oceanographic data consisting of conductivity, temperature, and salinity during this experiment is assessed and problem areas are investigated. These findings are presented in Chapter III and the AOSN II exercise is discussed later in this chapter.

B. BACKGROUND

1. Overview of the REMUS AUV

a. Characteristics

The following table lists the basic physical characteristics and operational limits of the REMUS AUV. This information was found in Hydroid, Inc. (2003).

Table 1. REMUS Characteristics

REMUS Parameter	**SI**	**English**
Length	158 cm	62 in
Diameter	19 cm	7.5 in
Dry Weight	36 kg	80 lbs.
Transit Depth Limit	100 m	328 ft
Operating Depth Band	3 m - 20 m	10 ft – 66 ft
Speed Range	0.25 m/s – 2.8 m/s	0.5 kts - 5.6 kts
Max. Operating Water Current	1.0 m/s	2 kts
Endurance	20 hours at 3 kts (1.5 m/s) 9 hours at 5 kts (2.5 m/s)	

b. Navigation

The REMUS AUV has three different navigation modes. These are long baseline, LBL, ultra short baseline, USBL, and dead reckoning, DR. Both LBL and USBL utilize submerged transponders, as discussed below. During these modes, if REMUS is unable to navigate successfully, due to poor acoustics, for example, it will default to the DR mode (Allen et al., 1997).

The LBL navigation mode uses acoustic transponders as reference beacons. The position of these transponders is designated in the mission program in latitude and longitude. During the mission, REMUS interrogates the transponders and they reply. The amount of time between an interrogation and the response is used to

determine range to a transponder. Each transponder uses a different frequency band so that REMUS can discriminate between them. REMUS also determines the speed of sound in water from data obtained via its CTD probe, and this data is used in the range calculation. The CTD probe will be discussed further in the Sensors section.

Once it receives the reply from a given transponder, the vehicle knows that its position is along the perimeter of a circle with the radius of the determined range from that transponder. In order to get a "good" navigational fix, REMUS must receive a reply from at least two transponders. In this way, the intersection of the two circles of known distance from the transponders "fixes" the vehicle's position. Then, because it knows its location with respect to the transponders and where the transponders have been placed on the Earth, the vehicle can determine its location in an Earth fixed frame (Matos, Cruz, Martins, & Pereira, 1999).

In a typical mission used for area search, REMUS drives a pattern of many parallel rows, henceforth referred to as "mowing the lawn", and two transponders are used. The line formed by these transponders is referred to as the "baseline". Obviously, there will usually be two intersections of the circles of detected transponder range. REMUS will accept the fixed position that is on the correct side of the baseline, as indicated by the programmed vehicle track (Hydroid, Inc., 2003). A diagram of a typical area search mission follows. DT1A and DT1B are the acoustic transponders.

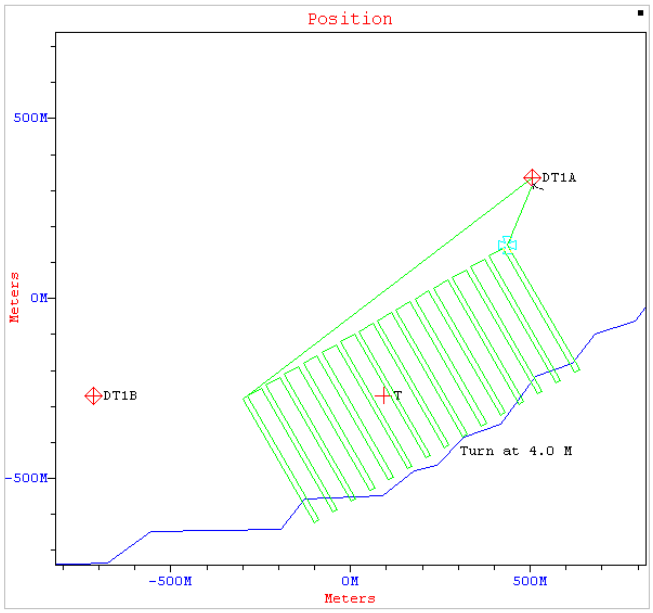

Figure 1. Typical Area Search Mission

USBL is a navigation mode that allows the vehicle to home in on a single transponder. This is made possible by a four-channel hydrophone that is located in REMUS' nose cone. The hydrophones are arranged in a cross pattern and are able to measure both range and bearing to a transponder. So, this mode is well suited for bringing REMUS to a given transponder at the end of a mission, in preparation for recovery. It can also be used for docking the vehicle (von Alt et al., 2001) but this has not been tested at the Naval Postgraduate School.

The DR mode of navigation determines position by taking the vehicle's last known position and adding the change in position, based on speed and heading. Heading is based on inputs from the vehicle's compass and yaw rate detector. The vehicle's speed is determined from a combination of ADCP measurements and turn rate of its propeller. The Acoustic Doppler Current Profiler (ADCP) can

very accurately measure the vehicle's actual speed over ground. It will be discussed further in the Sensors section.

Because the ADCP can sense the vehicle's speed over ground, DR navigation is more accurate when the vehicle is within its maximum range of 20 meters (Hydroid, Inc., 2003). The navigational accuracy is 1% to 2% of the distance traveled for both along and cross track error. The DR mode is far less accurate when speed is based on propeller turns. This is due to inaccuracies in speed measurement due to effects of current. Leonard, Bennett, Smith, and Feder (1998) state "The principle problem is that the presence of an ocean current will add a velocity component to the vehicle which is not detected by the speed sensor" (p. 3).

Other methods of navigation for REMUS have been developed by Hydroid and some end-users. The REMUS used for this thesis was actually upgraded with Global Positioning System (GPS) navigation just before the last experiment. This is discussed in Chapter II. The *Isurus*, A REMUS class AUV operated by the University of Porto was modified to navigate from a completely different LBL system that made use of a Kalman filter (Matos, Cruz, Martins, & Pereira, 1999).

c. Sensors

The REMUS used for this thesis is equipped with the standard sensor suite. A brief description of each of the instruments used to collect environmental data follows. Some actual sidescan sonar results are discussed in Chapter II. Also, the CTD is discussed in more detail in Chapter III. Specialized sensor suites have also been successfully

field tested (Purcell et al., 2000) but, once again, this REMUS has the standard suite.

- CTD – Conductivity and Temperature Detector - It measures conductivity and temperature, which are used to determine water salinity. This data is recorded for post-mission analysis and is also used by REMUS to determine the speed of sound in water for use in LBL navigation.
- OBS – Optical Backscatter Sensor - It measures optical backscatter, or reflectance, of the water. This can be used as an indication of water clarity.
- ADCP - Acoustic Doppler Current Profiler – This sensor has four upward looking and four downward looking transponders that measure the velocity of water above and below the vehicle. Also, when the vehicle is close enough to the ocean floor (approximately 20 meters) the ADCP can measure speed over ground (SOG) and altitude. SOG is used for the DR navigation mode and altitude can be used for determining bathymetry and for controlling vehicle depth in the constant altitude mode.
- Sidescan Sonar – It is 900 kHz with a maximum range of 40 meters on either side of the REMUS and a ping rate that adjusts automatically based on vehicle speed (Marine Sonic Technology, LTD., 1991). The sonar consists of transducers mounted along the vehicle's sides that send out beams of sound energy perpendicular to the track. Internal electronics and a dedicated computer and hard drive are used to process and store the acoustic returns. The echoed

returns are used to determine range to objects based on time lag and their intensity is used to create an image of the sea floor. A higher intensity return suggests more reflective object composition, such as metal. Also, "shadows" cast by objects can be used to estimate their height. Stand alone software is used for post-mission analysis of the sidescan images.

REMUS also has instruments that collect data about the vehicle's state for control and system diagnostics purposes. These include the compass, yaw rate sensor, and battery voltage meter. Data from these instruments is stored during each mission and can be exported from the vehicle.

d. Support Equipment

A picture of the REMUS with its support equipment is below. The equipment is also described briefly.

Figure 2. REMUS and Equipment, after Hydroid, Inc. (2003)

- Ranger and Towfish – The Ranger reports range to the vehicle in meters. This request can be sent once or set to query every 10 seconds. Ranger can also be used to detect range to a transponder. This is a good check to perform after positioning the transponders, just before starting the mission. It can also be used to send commands for starting and aborting the mission or to return to the mission start point. The towfish is the submersible transponder used for the Ranger's communications.

- Rocky – A rugged, field capable laptop computer used to communicate with the vehicle for mission programming, data retrieval, and status indication. All of these operations are performed using the REMUS Graphical User Interface (GUI). The Rocky laptop can be connected to REMUS using serial or Ethernet cable. One especially important feature is the ability to view the mission "playback" after retrieving the vehicle. This allows the user to see the REMUS performance throughout the entire mission, including attitude, navigation response, all system status messages, and battery power.

- Transponders – Used by REMUS as acoustic navigational aids during LBL and USBL modes of navigation. They each have different operating frequencies so that they can be discriminated by REMUS. They are positively buoyant and are designed to operate at the midpoint of the water column.

- Power/Data Interface Box – It is used for higher speed connection between Rocky and REMUS. It is also used to charge the vehicle's batteries.

2. AUVs and Mine Hunting

The practice of mining waterways began in the American Revolution and is still employed in modern combat. Mine warfare (MIW) can be used defensively, as in a country mining international waters to form a boundary against enemy penetration, or offensively by mining an enemy's waters so that its vessels are unable to safely deploy. It is possible to launch mines from aircraft, surface vessels, and submarines.

MIW has two sides, though. Along with mining, there are also the methods of mine countermeasures (MCM). AUVs are rapidly proving their utility in the specific area of MCM known as mine hunting. These are the techniques of detection, classification, identification, and neutralization of mines. REMUS has already demonstrated success in actual field operations as an MCM asset during Operation Iraqi Freedom. Ryan (2003) states "Reports of this first wartime deployment of the REMUS AUV system indicate that it proved invaluable in conducting surveys in the vicinity of Umm Qasr" (p. 52). Also, REMUS AUVs have faired well in controlled testing with pre-positioned mine like objects (Stokey et al., 2001).

However, a simple area search mission using one REMUS vehicle is quite elementary compared to the potential future of MCM. This vision (Rennie, 2004) involves teams of AUVs searching large areas in tandem and passing their results to other AUVs via underwater communications. These

follow on vehicles would then investigate the potential mines, classify and identify actual mines, and convey their findings to yet another set of AUVs. This final group would be specially equipped to neutralize the mines. All of this would be able to continue for extended periods with little or no human intervention since the AUVs would have advanced decision making capabilities and could recharge their batteries from a "mother vehicle" that would powered by an air breathing engine.

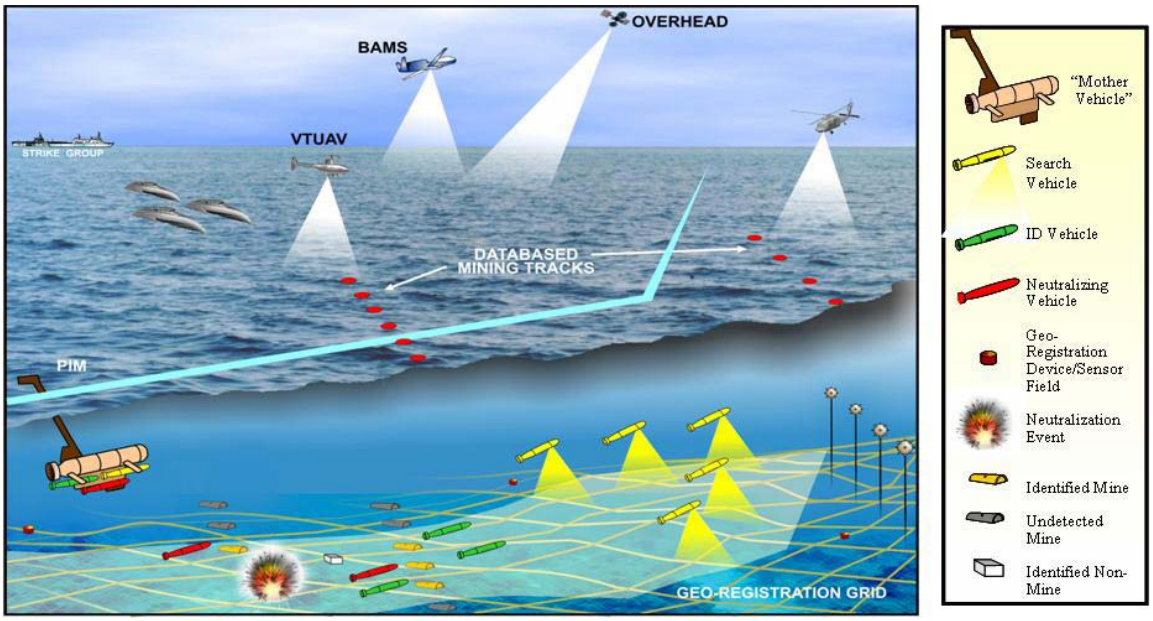

Figure 3. Vision of Future MCM, from Rennie (2004)

The plausibility of a vision such as this is contingent upon a number of advances in various technologies. The development of the artificial intelligence alone is daunting. However, even with these potential boundaries, the importance of accurate contact localization is obvious for the current state of the art in MCM and whatever the future may hold.

3. AOSN II

AOSN, which stands for Autonomous Ocean Sampling Network, is a project that was designed to use ocean sampling platforms to obtain higher resolution surveys than were possible using standard sampling methods (Curtin, Bellingham, Catipovic, & Webb, 1993). The reason higher resolution surveys were important is that they could be used to validate numerical models used for prediction of future ocean conditions. The way this would be possible is through the use of a combination of AUVs, point sensors, and acoustic sensors.

AUVs provide two main strengths. First, their autonomy makes them very well suited for collecting data over large areas, unlike moored sensors or buoys. They can also acoustically transmit data in almost real time to moored acoustic sensors. These sensors can transmit this to a central command post that could adjust the sampling tracks of the AUVs, as required, to ensure the most important data was being collected. This ability to dynamically direct the network of sampling platforms is referred to as "adaptive sampling" (Monterey Bay Aquarium Research Institute, 2004).

AOSN II is the second field test of the AOSN program. It was run by the Monterey Bay Aquarium Research Institute (MBARI). The main purpose was to study upwelling features in the Monterey Bay (Monterey Bay Aquarium Research Institute, 2004) and to demonstrate the improvement to ocean prediction models obtained by adaptive sampling. It took place from mid July to early September 2003.

THIS PAGE INTENTIONALLY LEFT BLANK

II. MINE DETECTION EXPERIMENT

A. PURPOSE

The REMUS AUV has already proven to be a good tool for detecting mine like objects in both experimental testing and actual missions. The main purpose of this experiment was to determine the repeatability of the vehicle's detection results. In other words, this experiment seeks to measure the variability of REMUS' contact localization ability. The precision of the localization results is also investigated. In order to be useful the detection system should be able to localize a mine like object (MLO) to within 10 meters so that another asset could reacquire and neutralize if needed.

B. DESIGN

1. Assumptions

The series of experiments were designed to test the variability of the detection position results for a given MLO. So, each experiment needed to be run under conditions that were very close to those during an actual area search mission. Also, in order to generate enough data to perform relevant statistical analysis, the "typical mission" detection of the given MLO needed to occur many times during an experiment. To this end, the assumptions for the experiments were as follows:

- During a typical mission the MLO is detected in one sidescan sonar image.
- The same operator analyzes the sidescan sonar data for the mission (every time it is simulated in the experiment).

- The mission is run with the same vehicle parameters (5 knots speed and 3 meters altitude).
- The sidescan sonar range is always the same for the mission (30 meters).

In normal operation, it is quite possible that the analysis of sidescan sonar images could be performed by different operators after different missions. However, this experiment was designed to compare the disparity in location of an MLO detected from a single mission. So, the assumption of a single operator was valid.

The vehicle parameters and sidescan sonar range chosen are also within normal operating limits. The range chosen was based on being able to detect an object of 1 meter in size or smaller (Hydroid, Inc., 2003). Altitude should be 10% of the sidescan sonar range. So, a 3 meter altitude is correct for a 30 meter sonar range. Also, for this sonar range a speed band of 2.6 knots to 5.1 knots is recommended, so that the along track resolution of the sonar image is limited to less than 1 meter. A lower vehicle speed could be used based on this band and/or to extend battery life. However, the experiment was run using 5 knots because this allowed for greater data collection rate and gave conservative results.

2. Development and Execution

As indicated above, the intent of the design was to maximize the data collection rate while maintaining the characteristics of a typical area search mission. Further, the data collected was to be analyzed statistically. To satisfy these requirements, the experiment was designed so that the REMUS would make multiple passes of the MLO. During each of these, the same approximate distance would

be maintained. Also, REMUS would be running under constant operating conditions, as detailed in the Assumptions section. The only intentionally varying parameter is the actual time each specific sample is taken. If no errors in navigation were present, the variance in MLO position would be due only to sidescan sonar errors and operator inconsistency in analyzing the sonar images, which should be minimized by using the same operator for each experiment.

Of course, there are navigation errors present that contribute to the measured position variance of the MLO. However, one of the biggest of these errors, transponder placement inaccuracy, is eliminated. This is because the data for a given mission is collected during a single experiment. Although the repeatability of a given mission's results is tested many times during the experiment, the transponders are deployed in the same location throughout. The transponders do move about their respective watch circle radii, but this variance is small.

In order to enhance the realism of the typical mission MLO detection, it was decided to use actual replicas of foreign mines, referred to as mine shapes, for the experiment. Shapes for a PDM 1, PDM 3, MK 44 Mod 0, and MK 45 Mod 1 were obtained from Mobile Mine Assembly Unit One (MOMAU 1). These were to be transported to the area of the experiment and placed. However, based on limitations of the handling equipment aboard the research vessel, it was determined only the PDM-1 shape could safely be deployed. This mine shape is pictured below.

Figure 4. PDM-1 Mine Shape

A diagram of the programmed vehicle route for the experiment follows. The vehicle first proceeds to point A, drives a rectangle pattern around the MLO 5 times, goes to Start Point, and then mows the lawn for 12 rows finishing the mission at DT1B. The rectangle pattern portion was to provide the AUV ten opportunities to obtain sidescan sonar images of the MLO. Mowing the lawn was included to have a good comparison of an image obtained during a typical area search with those obtained from the rectangle pattern portion.

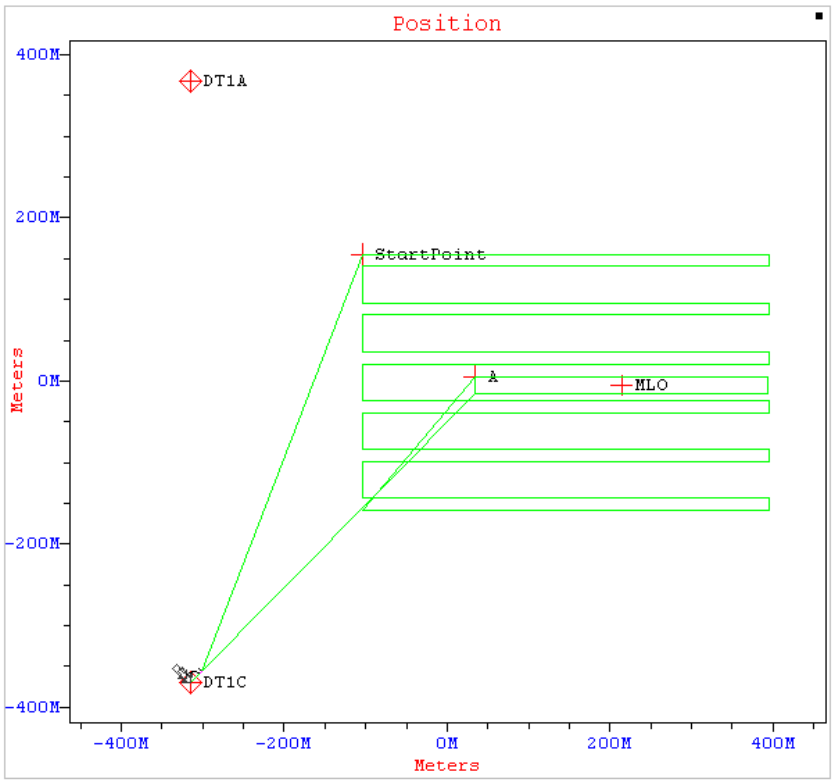

Figure 5. Initial Mine Detection Experiment Diagram

This version of the experiment was run as Mission 22. Unfortunately, this mission yielded only a few data points. The main problem was that the vehicle had no good acoustic navigational fixes until half way through the fourth rectangle. Because of this poor navigation, REMUS was actually driving rectangles around a different area that did not include the MLO. Although it did obtain sidescan sonar images of the MLO during the 3 remaining passes of the rectangle phase and once while mowing the lawn, the mission was still deemed a failure.

During post-mission analysis, it was noted that the vehicle received many more good acoustic fixes during its lawn mowing phase. Based on this realization, the experiment was modified such that the vehicle mowed the lawn before it drove the rectangles. The theory was that it

would have far greater opportunity to obtain a number of good fixes, thus minimizing its position error, before the rectangle phase. Also, the number of rectangles was increased to 10 in order to further improve the potential for acquiring sidescan sonar observations of the MLO.

This version of the experiment was run as Mission 23. It was more successful than Mission 22 in that the number of images of the MLO increased to 7. However, this was still 13 less than the maximum possible during the rectangle pattern phase. Further, 1 or 2 images from mowing the lawn were also expected. Unlike Mission 22, the problem with this mission was not poor navigation but placement of the MLO. The vehicle drove the programmed rectangles but the MLO was not positioned inside of them.

The third and final version of the experiment was designed. The navigation pattern was maintained the same as Mission 23. The difference was that instead of using a mine shape as the MLO, a bottom mounted oceanographic instrument suite was used. This suite was constructed and deployed by the Department of Oceanography at the Naval Postgraduate School and is named the Monterey Inner Shelf Observatory (MISO) (Stanton, 2003). The photographs following show the MISO before deployment and an aerial view of Monterey Bay indicating its location. The MISO is approximately 1 m tall after mounting.

Figure 6. MISO Prior to Deployment, from (Stanton, 2003)

Figure 7. MISO Location, from (Stanton, 2003)

The advantage of using MISO as the MLO was that it was already deployed. So, the ability to accurately place the PDM-1 mine shape for an experiment was unneeded. This meant that as long as the vehicle was receiving good navigational fixes during the mission, it would be considerably easier to drive rectangles around the MLO.

The diagram of the programmed vehicle route for the final version of the experiment, Mission 26, is below. There are only two substantial differences between Missions

23 and 26. One is that the former had the legs of the rectangle on 090° and 270° courses while the latter has them on 140° and 320°. This is due to the change in the curvature of the coastline between the areas where the two missions were performed. Secondly, the number of rectangles was increased to 15 for Mission 26. This is to further increase the opportunity of the REMUS to obtain sidescan images of the MLO.

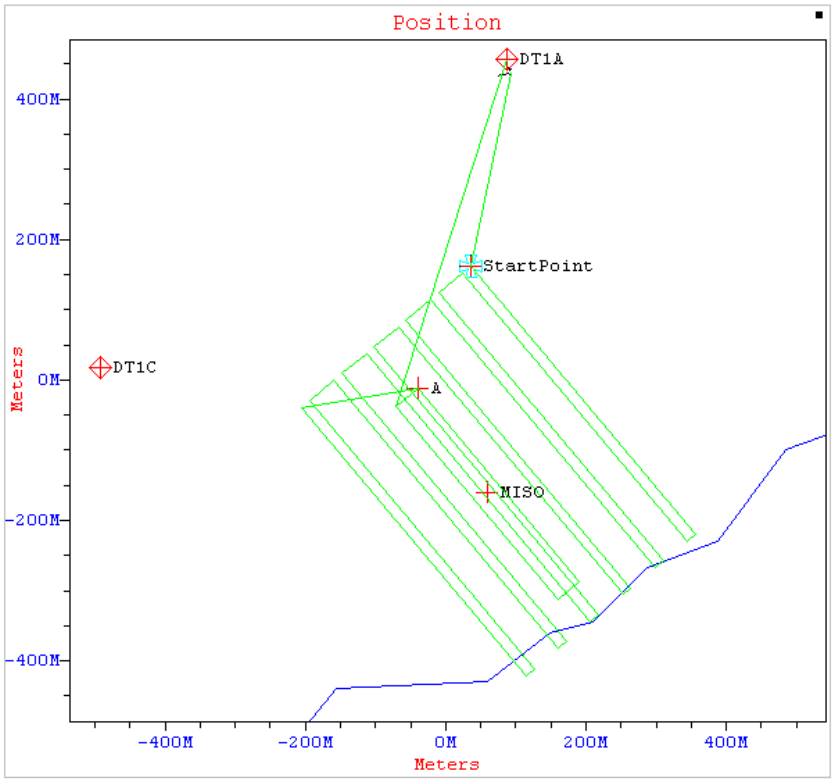

Figure 8. Final Mine Detection Experiment Diagram

C. RESULTS AND ANALYSIS

A plot of the vehicle's track during the rectangle portion follows. The detected MLO positions and the "actual" position of the MISO lab are shown inside the rectangular track. It is very difficult to know the exact position of the MISO lab since it is submerged in roughly 10 fathoms (60 feet or 18.3 meters) of water. An

approximate location is known from diving on the lab, releasing a buoyant marker, and obtaining its GPS position.

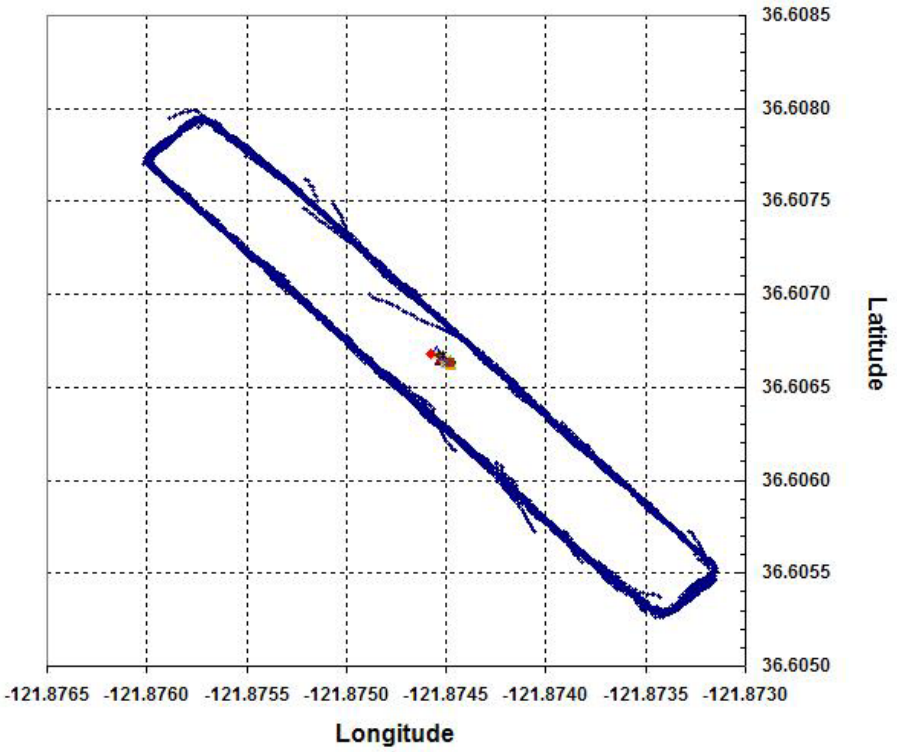

Figure 9. Mission 26 Rectangle Portion

This version of the experiment was very successful. The REMUS obtained 31 sidescan sonar images of the MLO. There were 30 from the rectangle portion and the other was from mowing the lawn. A portion of one of these images showing the MISO lab is below. Also, a plot of the detected MLO positions and the corresponding REMUS positions follows. Most of the plotted points are actually multiple points at the same position. Therefore, only 17 REMUS position markers and 13 MLO markers are shown. As indicated, the positions for the 320° leg are in blue and those for the 140° leg appear in red.

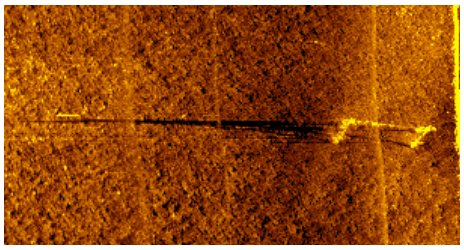

Figure 10. Sidescan Image of MISO Lab

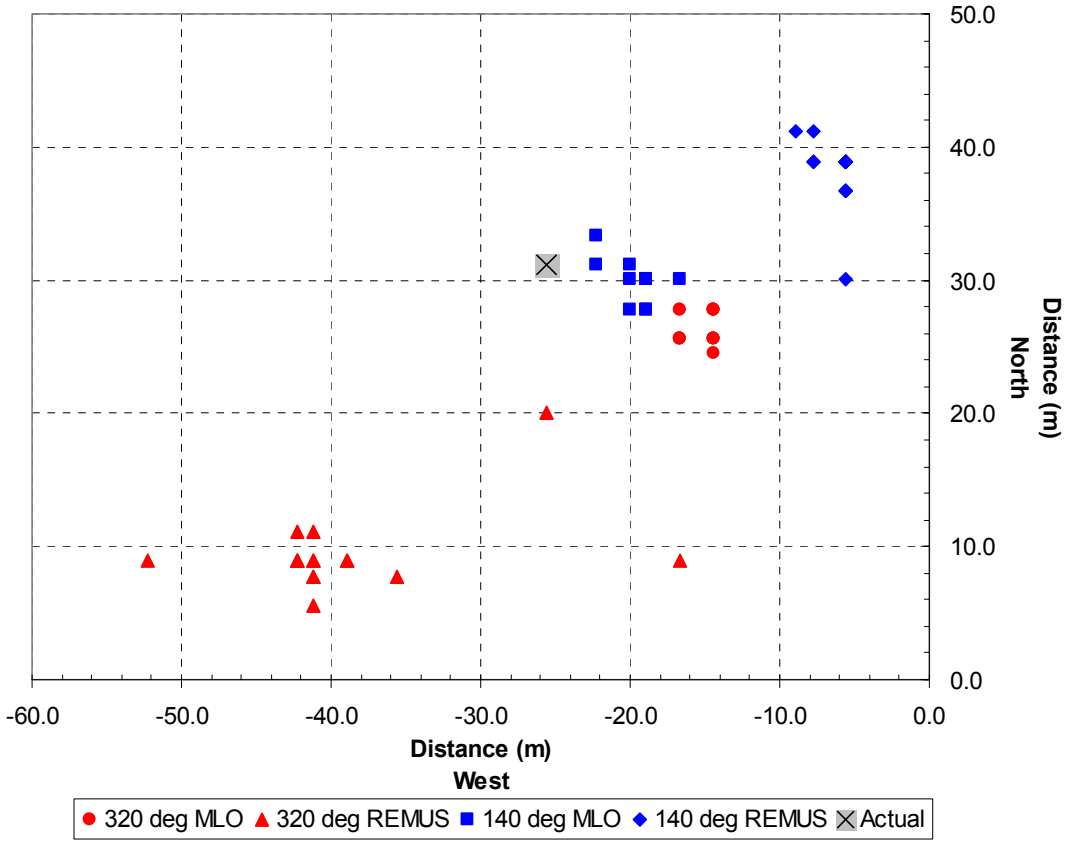

Figure 11. Mission 26 Results

The Mission 26 experiment showed several different results. In some cases, the same detected position for a given mine was obtained at different vehicle locations, showing a location independence to the results. In one situation, the same MLO position was detected for four different vehicle positions, two of which were over 30 meters apart. Below is a plot of only the 320° leg results

with these data points shown in green. Location independence for MLO position results is obviously desirable for an AUV used to perform area searches.

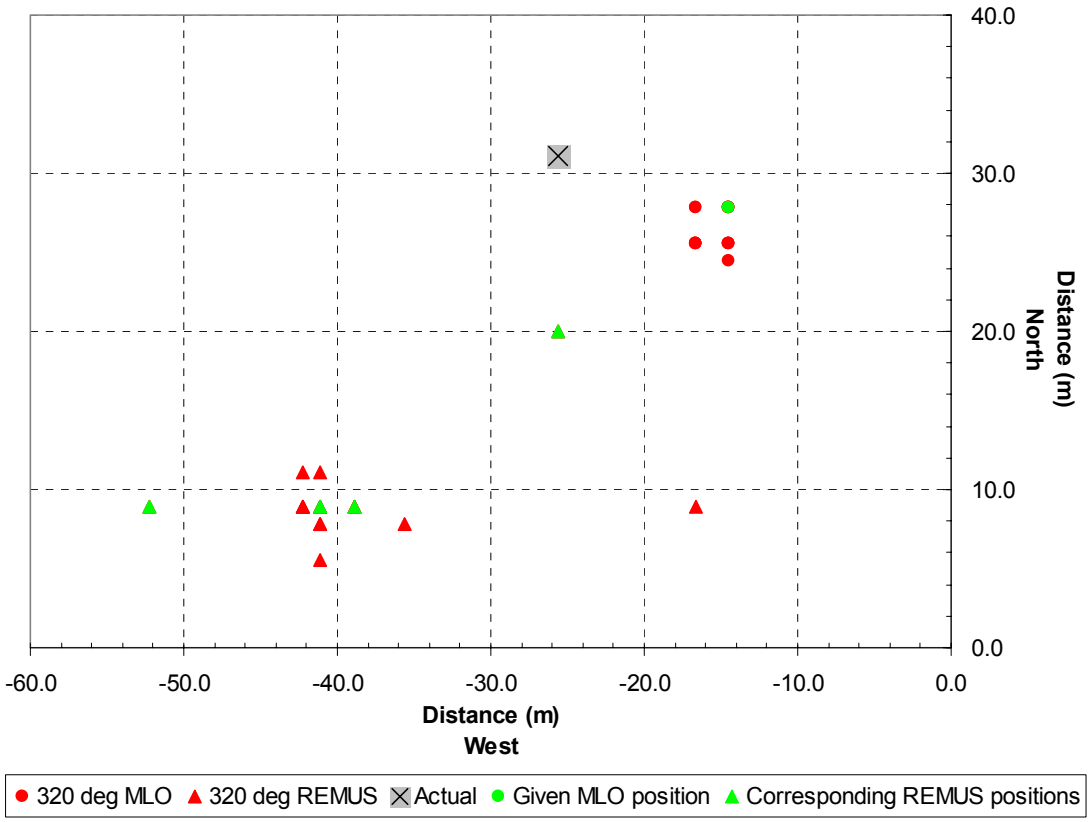

Figure 12. Example of Location Independence to Data

Unfortunately, this result did not always hold true. In some cases, the same REMUS location yielded different MLO positions. The greatest distance between MLO positions from the same REMUS location is 3.52 meters. This is undesirable.

By far the most significant result is the apparent course dependency for detected MLO position. There is a definite separation between the clusters of data from the two different legs. This implies that during normal lawn mowing searches the detected position of the same mine

could vary based on which leg it was detected. The separation between the mean values for each leg was 5.38 meters and that for the extreme (outlying) positions was 11.8 meters.

In order to further analyze the data scatter of the detected MLO positions, the coordinate system was rotated such that the vertical axis would be in the direction of the REMUS heading during the rectangle portion of the experiment. This was done for both the 140° and 320° headings. The calculations were as follows.

$$x' = x\cos\theta_{x'x} + y\cos\theta_{x'y}$$
$$y' = x\cos\theta_{y'x} + y\cos\theta_{y'y} \qquad (1), (2)$$

Where: x is the original x-axis.

x′ is the new x-axis.

y is the original y-axis.

y′ is the new y-axis.

$\theta_{x'x}$ is the angle between x′ and x.

$\theta_{x'y}$ is the angle between x′ and y.

$\theta_{y'x}$ is the angle between y′ and x.

$\theta_{y'y}$ is the angle between y′ and y.

Next, the new coordinate systems were translated to the centroid of their respective data set. The resulting plots are below. It can be seen that the data is now plotted in such a way as to clearly display the along track and cross track variance. The standard deviation, σ, of each component of the data is indicated on the plots. Once again, many of the plotted points actually have more than one MLO detection location plotted on top of each other.

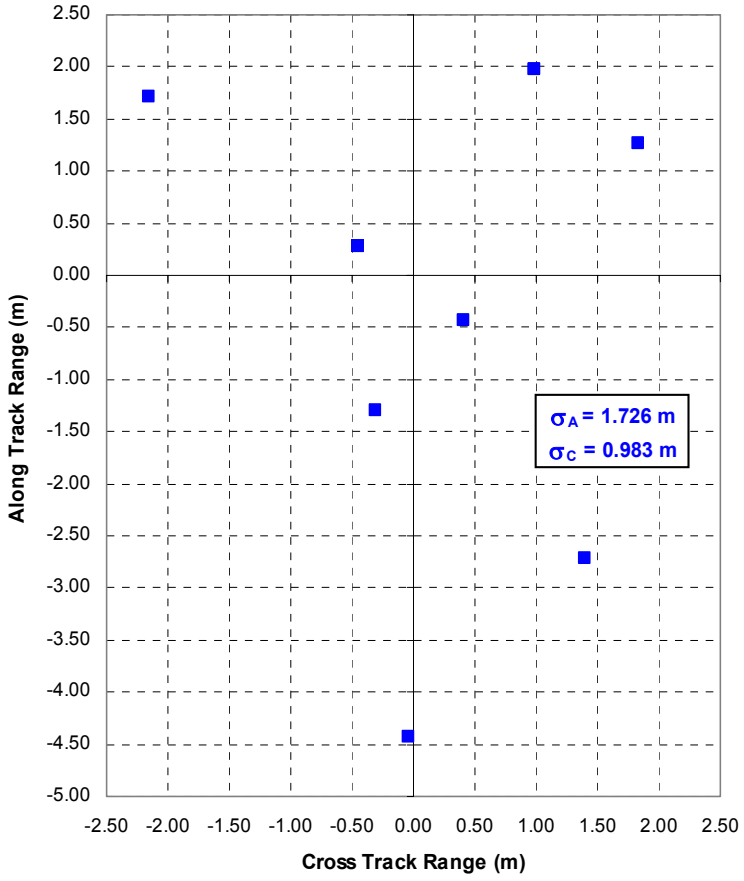

(a)

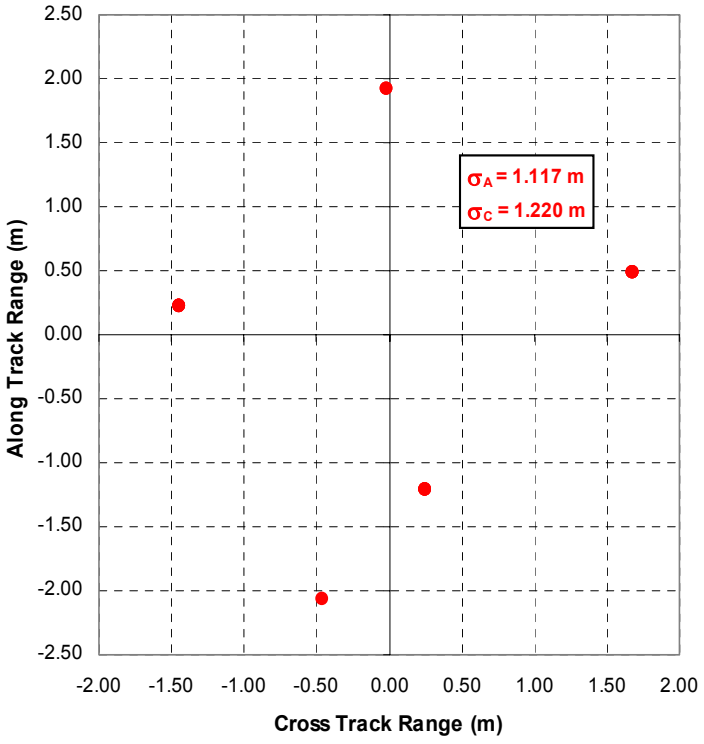

(b)

Figure 13. Mission 26 Data Variance (a) 140° Leg (b) 320° Leg

These plots indicate an obvious difference in the data variation. In the 140° leg data there is an almost 2 to 1 ratio of standard deviation of the along track component of the data to that of the cross track. Conversely, the 320° leg results have almost equal values for along and cross track standard deviation.

The experiment was run again in order to test its repeatability. This was first attempted during Mission 27, which had to be terminated roughly one third of the way through because the REMUS became bogged down in a kelp bed. Fortunately, the vehicle floated to the surface and was easily retrieved by a swimmer.

Mission 28 was then conducted, once again, to validate the results from Mission 26. First, the Mission 27 playback was viewed to determine the point at which the vehicle became entangled in kelp. It was clear that this happened while it was still mowing the lawn. Also, a rough outline of the kelp bed perimeter could be determined by watching the vehicle's attitude in the REMUS GUI. It was noted that the rectangle portion of the search area appeared to be free of substantial kelp interference while the majority of the lawn mowing portion did not. Based on this determination, it was decided to run the experiment with just the rectangle portion.

Results from Mission 23 had indicated that mowing the lawn prior to the rectangle phase was important to give REMUS ample opportunity to get some good acoustic navigation fixes. The vehicle would then have a much higher probability of driving rectangles in the right place. However, between Missions 26 and 28 the REMUS had been upgraded with a GPS navigation system. It would now have

good navigation information up until submergence, when the GPS antenna would be unable to receive satellite information. Therefore, even if acoustic navigation was poor during the submerged transit to the start of the rectangle phase, the vehicle would still have a very good chance of dead reckoning to the correct location.

Plots of the data from this mission follow. The coordinate system was rotated and translated in the same manner as in Mission 26 for the variance plots.

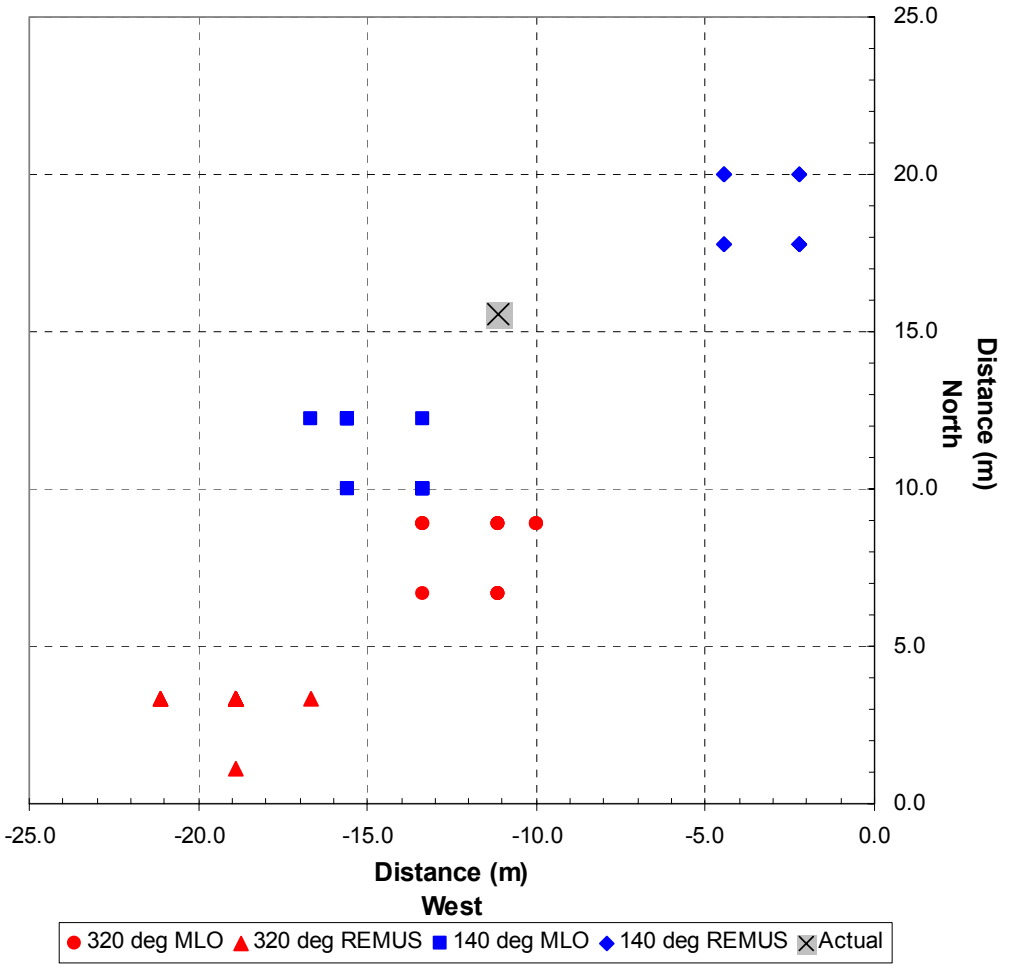

Figure 14. Mission 28 Results

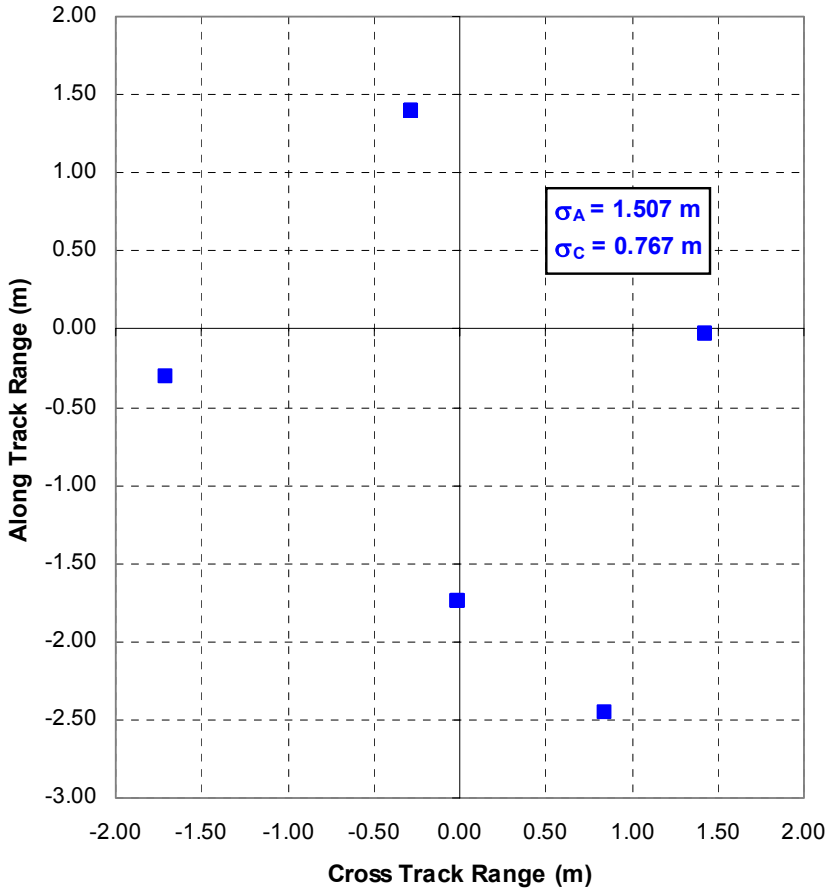

(a)

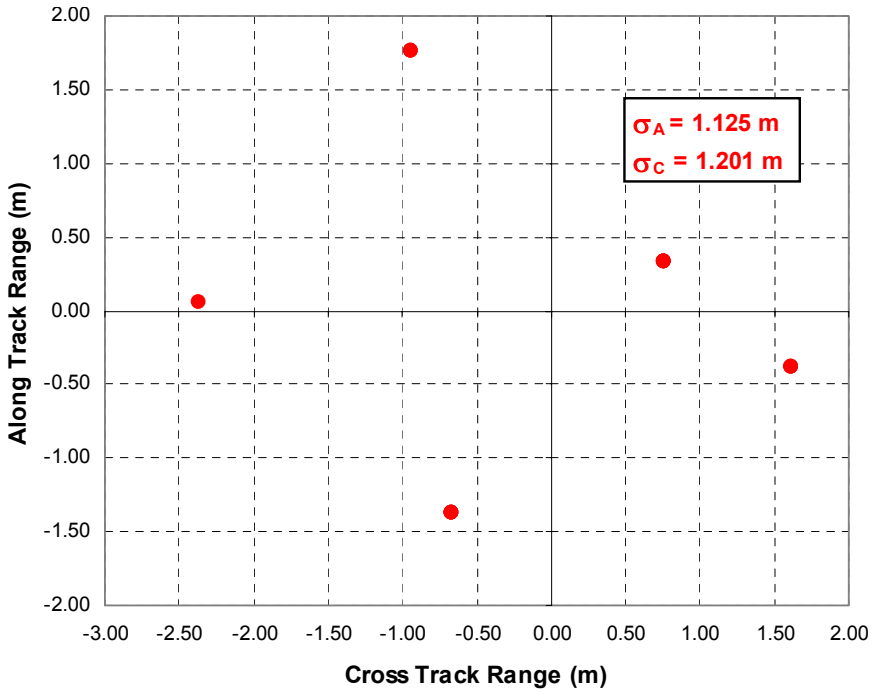

(b)

Figure 15. Mission 28 Data Variance (a) 140° Leg (b) 320° Leg

The results of Mission 28 were very similar to those of Mission 26. There was, once again, a clear separation between the grouping of detected MLO positions from the 140° and 320° legs. Also, the standard deviations displayed comparable behavior. The ratio of σ_A to σ_C for the 140° leg was again near 2 to 1. Further, the values for the 320° leg data were quite close to those from Mission 26. The table below summarizes these results in percent error, as defined by the following equation.

$$\% \, Error = \frac{|x_{26} - x_{28}|}{x_{26}} \times 100\% \qquad (3)$$

Where: x_{26} is the variable value for Mission 26.

x_{28} is the variable value for Mission 28.

Table 2. Comparison of Results From Missions 26 and 28

	140° leg			**320° leg**		
	σ_A (m)	**σ_C (m)**	**Ratio σ_A : σ_C**	**σ_A (m)**	**σ_C (m)**	**Ratio σ_A : σ_C**
Mission 26	1.726	0.983	1.756	1.117	1.220	0.916
Mission 28	1.507	0.767	1.965	1.125	1.201	0.937
% Error	12.8	22.0	11.9	0.7	1.6	2.3

The major difference between the two missions is that the REMUS seems to have had better acoustic navigation during Mission 28. This is indicated by the tighter grouping of REMUS position markers in Figure 14 as compared

to Figure 11. In order to verify this apparent result, each individual rectangle leg, 140° and 320°, driven for both missions was analyzed for the number and character of its acoustic navigation fixes. The table below clearly indicates that the acoustic navigation was much better during Mission 28. In addition, a qualitative analysis of these rectangles shows that many of the areas where REMUS had poor acoustic navigation during Mission 26 were very close to the portion of the leg where the MLO was imaged by sidescan sonar. Hence, it is not simply a matter of having fewer good fixes during the Mission 26 legs but also that the lack of fixes tended to be in the direct vicinity of the MLO, where they would most affect the vehicle's ability to accurately detect its position.

Table 3. Average Number of Good Fixes

	140° leg	**320° leg**
Mission 26	29.1	31.1
Mission 28	42.0	42.4

The better navigational accuracy during Mission 28 improved the accuracy of the MLO position data. Standard deviation values decreased for all but the 320° leg along track results. These did have an increase but the error between the Mission 26 and 28 values was only 0.7%. So, the increase was not significant.

The superior navigation in Mission 28 did decrease the variance in detected MLO position. The distance between each leg's mean was 4.03 meters and the distance between the extreme positions was 7.9 meters. However, segregation

between 140° and 320° leg data did cause this distance to be higher than it otherwise would have been.

In Stokey et al. (2001), the results from mine detection testing had an average position error of 7.5 meters. This was considered small and attributed largely to GPS error. So, values of 11.8 meters and 7.9 meters between the outlying MLO positions for Missions 26 and 28, respectively, could also be considered small.

The tests are completely different, though. The test performed in 2001 was to determine what percentage of MLOs in a known test area would be found and with what accuracy. In the experiment for this thesis, the intent was to determine the repeatability of results for a given MLO over many runs. So, it is difficult to say that these results can be directly compared.

Also, even if the differences are not considered large, they are not due to GPS error. They are apparently due to a course dependency to the data. So, from an evaluation standpoint, their size is less important than their source.

THIS PAGE INTENTIONALLY LEFT BLANK

III. TEMPERATURE AND SALINITY MEASUREMENT

A. OVERVIEW

1. CTD Explanation

The REMUS AUV is equipped with a conductivity, temperature, and depth probe or CTD. This probe is a YSI Model 600XL. It is mounted in the nosecone of the REMUS so there will be flow over its sensors as the vehicle is propelled through the water. Software necessary for processing the probe's readings runs on the REMUS onboard computer. Temperature and conductivity information from the CTD probe is used for calculating the local speed of sound in water. This, in turn, is utilized during LBL navigation. CTD data is also stored on the REMUS hard drive for post mission analysis.

The CTD probe measures temperature via a sintered metallic oxide thermistor that changes in electrical resistance as temperature varies (YSI, Inc., 1999). This resistance change is predictable and is used by the probe's electronics to determine the water's temperature. Temperature data is recorded by the software in °C. The temperature accuracy of the CTD probe, while operating as installed in the REMUS, is +/- 0.15 °C (Hydroid, Inc., 2003).

Conductivity is measured from a separate portion of the YSI probe. This section has a cell with four pure nickel electrodes. Two of these are current driven, while the other two are used to measure voltage drop. The measured voltage drop is interpreted as a conductance value in milli-Siemens. This is converted to a conductivity value

in milli-Siemens per cm (mS/cm) by multiplying it by the cell constant in units of cm^{-1}.

In the laboratory, salinity can be measured directly from a sample of seawater by measuring the weight of the salt left behind after evaporating the water. However, this method has been found to be relatively inaccurate due to loss of some components during the drying process. Consequently, other methods that relate directly measurable properties of the seawater to its salinity level are often utilized. Such properties include the conductivity and the density.

The YSI probe software calculates the salinity from the temperature and conductivity using the algorithm detailed below. This algorithm is based on the salinity of standard seawater as related to the conductivity of a specific solution of KCl. Because of this, resulting values are unitless. However, the unitless salinity numerical values are very close to those determined from the standard method, in which the mass of dissolved salts in a given mass of water was determined directly. So, the output is reported in units of "ppt" or parts per thousand.

2. CTD Algorithm

The CTD probe's salinity algorithm is as follows. Coefficients a_n, b_n, c_n, and d_n, are specified in American Public Health Association (1995).

$$R = R_t * R_p * r_t = \frac{C(S,t,p)}{C(35,15,0)} \tag{4}$$

$$\rightarrow R_t = \frac{R}{R_p * r_t} \tag{5}$$

$$R = \frac{C}{42.914\, mS/cm} \tag{6}$$

$$r_t = c_0 + c_1 t + c_2 t^2 + c_3 t^3 + c_4 t^4 \tag{7}$$

$$R_p = 1 + \frac{p(e_1 + e_2 p + e_3 p^2)}{1 + d_1 t + d_2 t^2 + (d_3 + d_4 t)R} \tag{8}$$

$$\Delta S = \frac{(t-15)}{1 + k(t-15)}\left(b_0 + b_1 R_t^{1/2} + b_2 R_t + b_3 R_t^{3/2} + b_4 R_t^2 + b_5 R_t^{5/2}\right) \tag{9}$$

$$S = a_0 + a_1 R_t^{1/2} + a_2 R_t + a_3 R_t^{3/2} + a_4 R_t^2 + a_5 R_t^{5/2} + \Delta S \tag{10}$$

Where: R is the ratio of measured conductivity to that of the Standard Seawater Solution.
t is temperature in °C.
p is pressure above one standard atmosphere in bars (1 bar = 10^5 Pascals).
R_t is R as a function of t.
R_p is R as a function of p.
C(S,t,p) is the measured conductivity. It's a function of salinity, temperature, and pressure.
C(35,15,0) is the conductivity of the Standard Seawater Solution (42.914 mS/cm).
S is the calculated salinity value in ppt.

B. AOSN II RESULTS

1. REMUS AOSN II Mission Description

REMUS CTD data was collected over long transect missions during AOSN II. Several different missions were run but there were few differences between them. In each case, the vehicle was inserted in approximately 26 meters of water within 20 meters of one of the two transponders. After proceeding to a fixed starting point,

CC start, located at 36°41.823'N, 121°50.081'W, the vehicle was programmed to proceed down a straight line track at a bearing of 280° for approximately 9 nautical miles (16.7 km), turn, and follow the reciprocal track inbound. A diagram of the navigation plan is below.

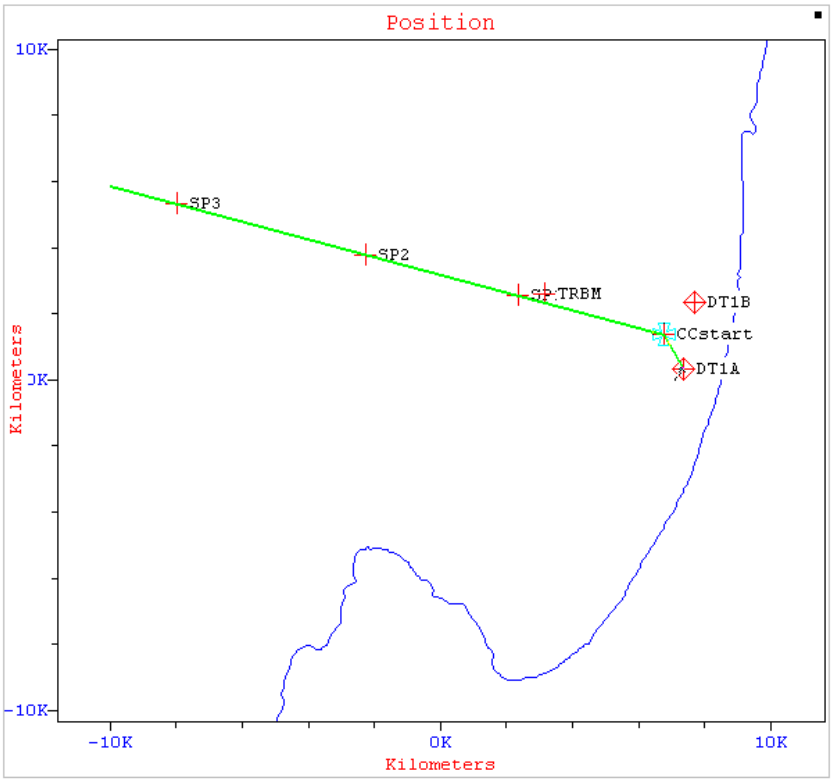

Figure 16. Mission 14 Navigation Plan

During the long transects, the depth keeping mode was set to "triangle" between 3 m and 50 m. This mode causes the vehicle to drive a saw tooth pattern between the minimum and maximum depths. The REMUS mission program also requires the ascent/descent rate for the vehicle to travel between the minimum and maximum depths. A depth rate of 6 m/min was used for the AOSN missions. This is well within usual XBT casts and is required to be slow enough that sensor response lags are negligible.

Data from all of the AOSN II missions was very similar. The specific data discussed in this chapter is from Mission 14, which was performed on 14 August 2003. The mission number is based on the total number of missions run at the Naval Postgraduate School using this vehicle. So, Mission 14 was only the third AOSN II mission. Its mission parameters are below.

Table 4. AOSN II Mission Parameters.

Date:	Aug. 14, 2003
Start time:	8:26:17.0
Duration:	3:52:12.6
Average velocity:	Meters/sec.:2.71 Knots:5.27
Mission length:	37782 meters 20.40 nautical miles
Distance traveled:	37780 meters 20.40 nautical miles
Power:	556.1 Watts used
Instruments:	RDI ADCP YSI CTD MS Sidescan Seatech OBS
Mission Parameters:	Legs 1 to 4 Alt: 3.0 (1677 rpm) Legs 5 to 7 Triangle: 50.0 (1677 rpm) Leg 8 Alt: 4.0 (1677 rpm)

2. Raw Data

The CTD data had some puzzling problems. Both the temperature and conductivity data were very noisy and had unexpected spiking around the points where REMUS transitioned from a positive to negative depth rate and vice versa. This pronounced fluctuation in the data was observable at every shift in depth rate but with varying characteristics. In some cases it was one or two very large spikes while at other times it was several smaller ones.

An example from the temperature results is shown below. Please note that the dashed line is the vehicle's depth and it is plotted such that depth is highest at the top of the plot.

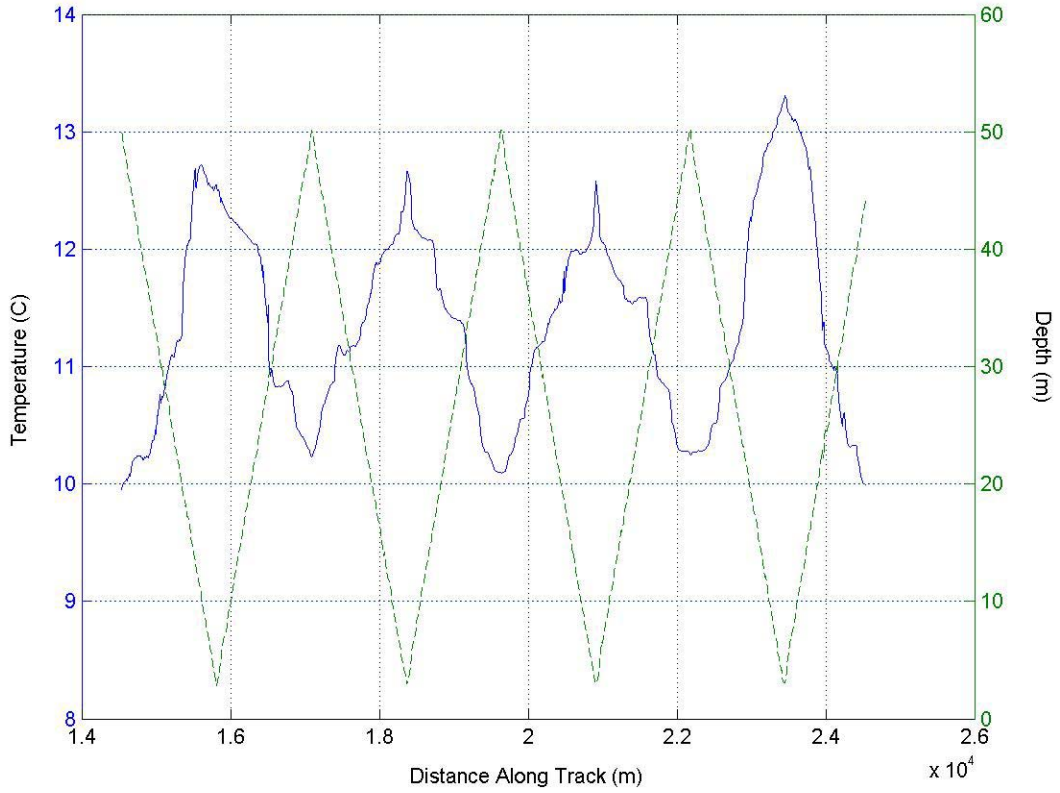

Figure 17. AOSN II Temperature Data Example

The spiking was more pronounced as the vehicle reached its minimum programmed depth, thus changing from diving to rising. This trend is apparent in all of the temperature and conductivity data collected during the triangle depth mode.

Since salinity is a function of temperature and conductivity its results displayed even more fluctuation than the others. A portion of the salinity results from Mission 14 is shown below. This plot shows that the salinity data displayed spiking very frequently throughout the mission. Once again, spiking was often more severe near a change in depth rate.

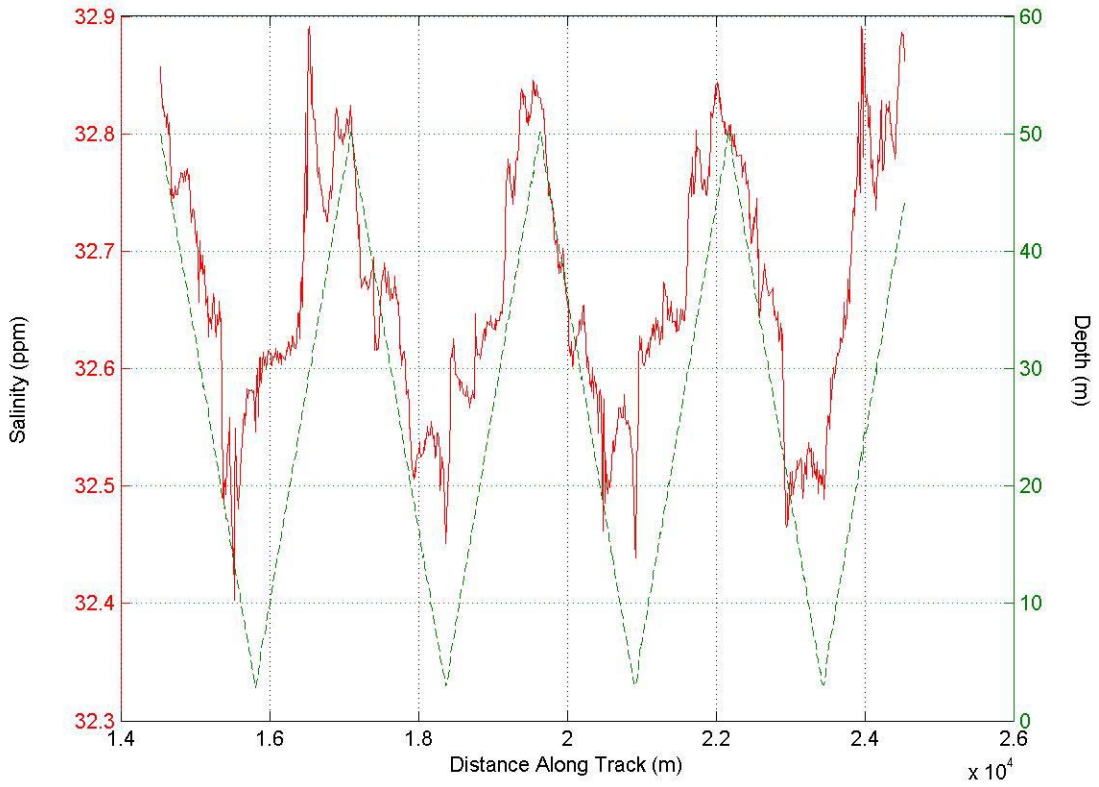

Figure 18. AOSN II Salinity Data Example

The salinity results and temperature data were used to generate two-dimensional contour plots. These plots were created using a combination of spline and Lagrange curve fitting of the data obtained by the vehicle as it drove a triangle depth pattern. Thus, the data obtained from points along the black lines, which show vehicle position, is used to generate plots of interpolated data for an entire "swath" of ocean.

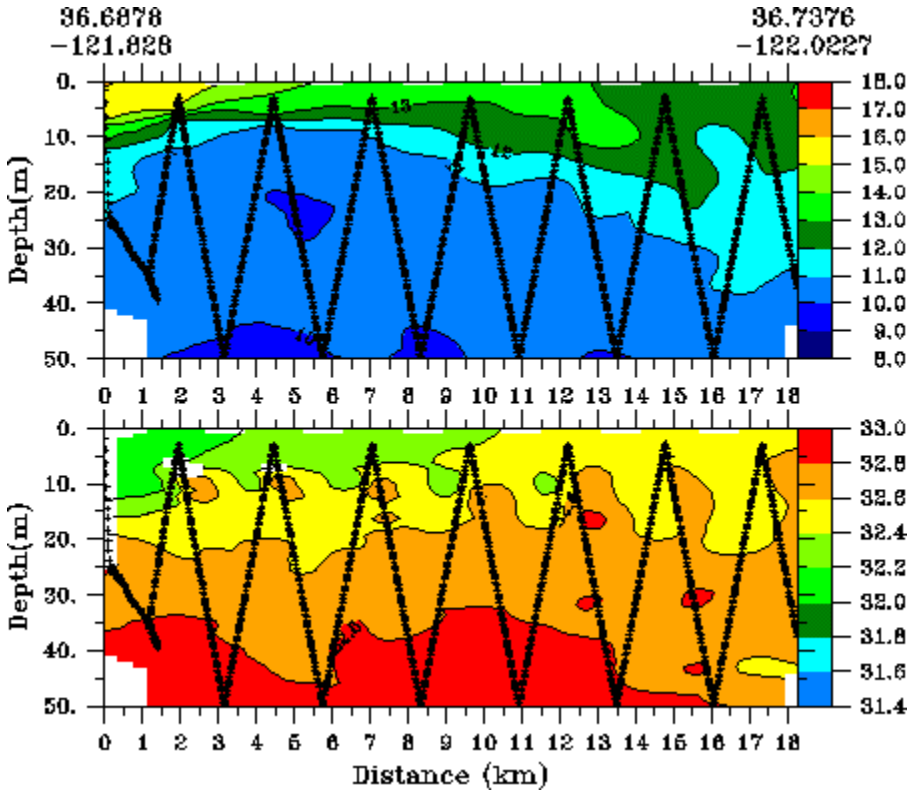

Figure 19. Mission 14 Outbound Track Raw Data (Note: Upper Plot-Temperature (°C), Lower Plot-Salinity (ppt))

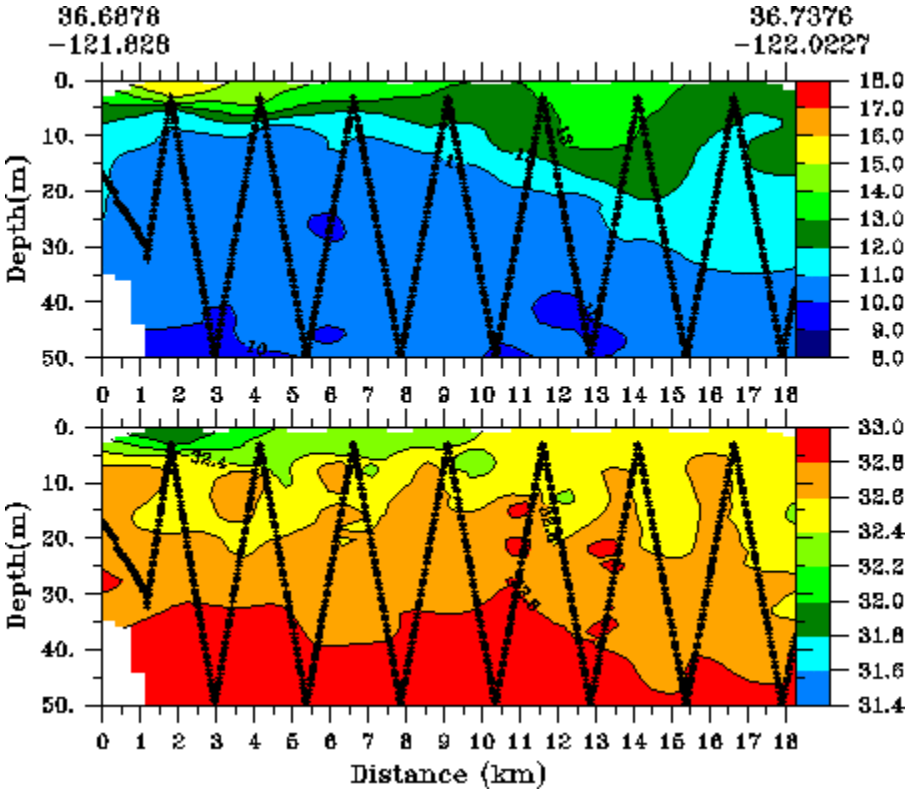

Figure 20. Mission 14 Inbound Track Raw Data (Note: Upper Plot-Temperature (°C), Lower Plot-Salinity (ppt))

Based on the problems with the CTD data already detailed, it is unsurprising that these contour plots also have some anomalies. For one thing, they do not display a smooth transition between regions. This is especially true for the salinity plots in the area where salinity increases from the 32.6 ppt - 32.8 ppt region to the 32.8 ppt – 33.0 ppt region. Along this boundary there are finger-like projections stretching from one region into the other. This characteristic does not correspond well with normal salinity and temperature profiles expected to occur in nature.

Another problematic feature of these plots is the "bubbles" of color from an adjacent region appearing in the current region. This is quite pronounced in the inbound

salinity plot at distances between 10.5 km – 14 km. Here, red "bubbles" appear all along the height of the orange band. It can also be seen that these "bubbles" appear to originate from the actual data values along the vehicle's position line.

3. Analysis of Raw Data

Since the raw data had apparent anomalies, some potential causes were investigated. These results are discussed later in this section. Concurrently with investigating possible error sources, the raw data was also mathematically smoothed. The purpose of this endeavor was an attempt to filter out noise, leaving behind only accurate values.

The boxcar algorithm was used. It is a method for smoothing data by using the average of several data points in place of each individual point. A user defined value, m, is utilized to determine the number of data points before and after the current data point to be used in the averaging. The boxcar algorithm appears below.

$$x_n = \frac{x_{n-m} + x_{n-m+1} + .. + x_n + .. + x_{n+m-1} + x_{n+m}}{2 * m - 1} \qquad (11)$$

Where: n is the current data point.
m is a user defined value.

The following plot shows a comparison of three different m values. It can be seen that as m increases, the curve becomes smoother, as expected. This is good because the algorithm is removing more noise. However, too large a value of m can cause actual trends to be smoothed out. Thus, the green trace, corresponding to m=30, seems to have

the best combination of reduced noise with a good representation of the actual data.

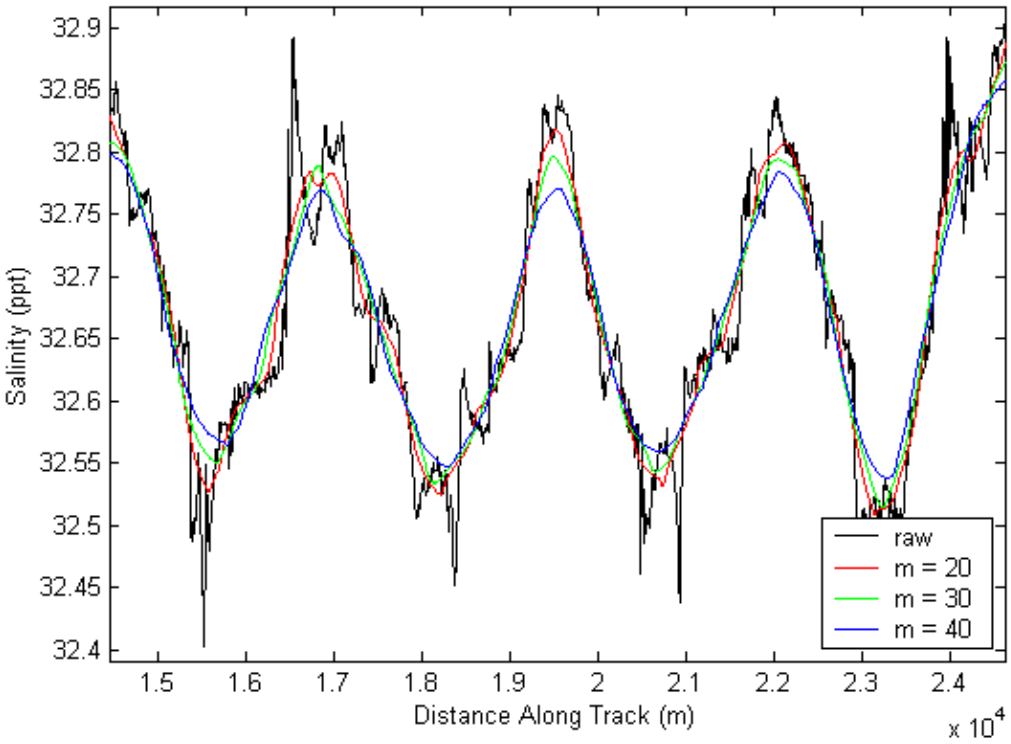

Figure 21. Boxcar Algorithm m Value Comparison

The smoothed salinity data obtained using m=30 was then utilized to generate two-dimensional contour plots, as before. These plots appear below.

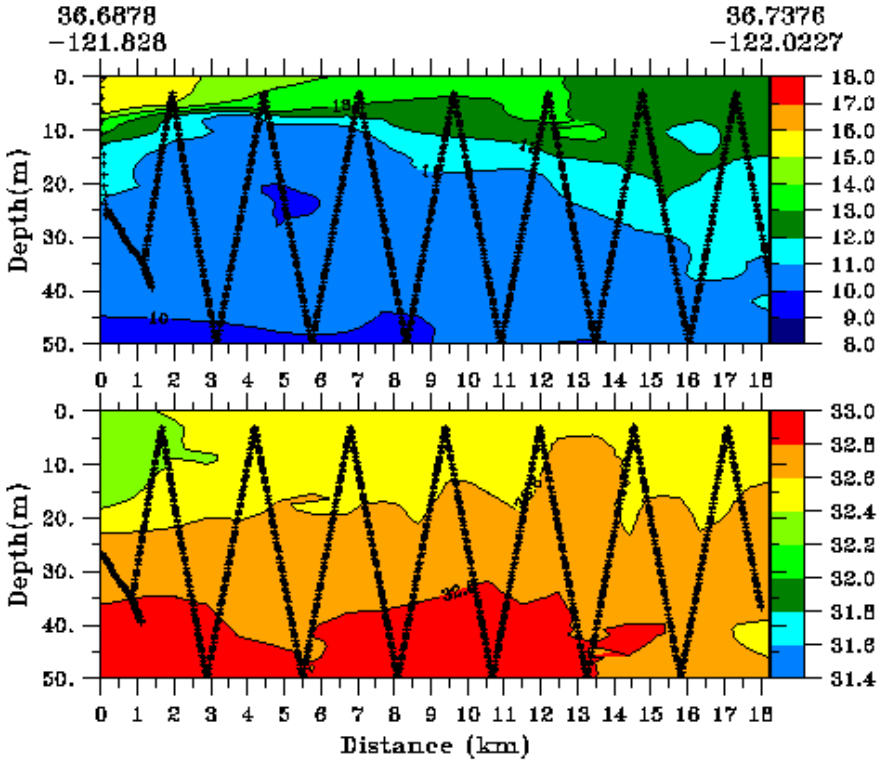

Figure 22. Mission 14 Outbound Track Smoothed Data (Note: Upper Plot-Temperature (°C), Lower Plot-Salinity (ppt))

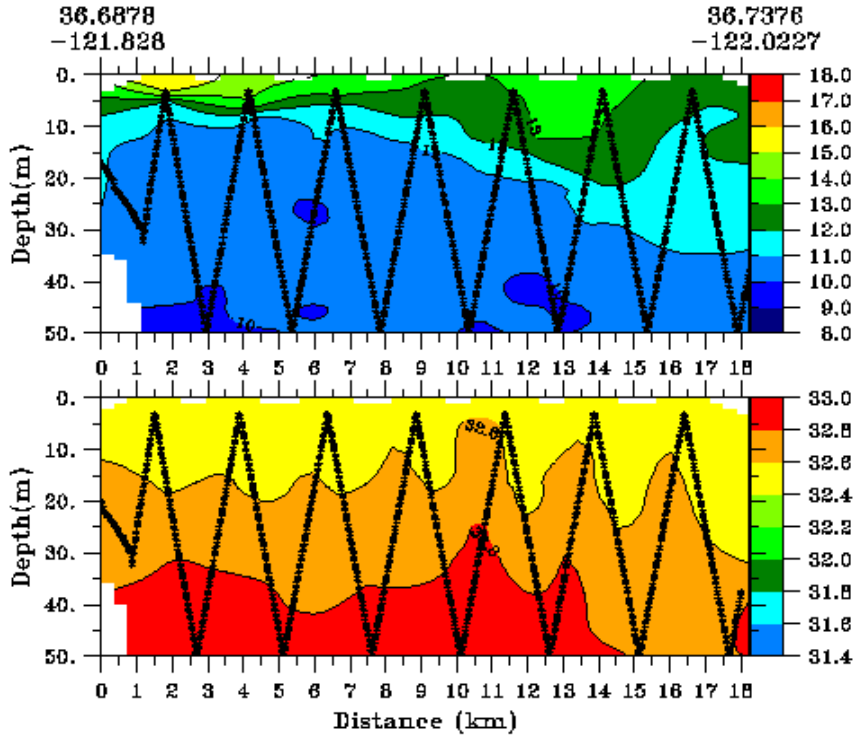

Figure 23. Mission 14 Inbound Track Smoothed Data (Note: Upper Plot-Temperature (°C), Lower Plot-Salinity (ppt))

The contour plots of smoothed salinity were somewhat better than those of the raw data. One definite improvement was the lack of "bubbles" of color in an adjacent color area. However, the jagged transition between regions was still present. Smoothing the salinity data had made an improvement but the results were still rather poor. The character of the instrument's sampling path (triangle) should not appear in the data if correct sampling is occurring.

a. CTD Probe Time Offset

A potential problem with the CTD probe could have been a time offset between the temperature and the conductivity sampling. Thus, a given temperature data point could be taken from a slightly different time than its corresponding conductivity data point as used in the salinity calculation. This offset would, in essence, mean that temperature and conductivity values used in a given salinity calculation could be from two different vehicle positions. This is obviously not taken into account in the salinity calculation, detailed above.

In order to explore this potential source of error, the correlation coefficient was calculated for the temperature and conductivity data. Then, the conductivity data was shifted such that for a given temperature data point at sample time t, the corresponding conductivity data point was at time t+1 with respect to the original data set. The correlation coefficient for temperature and conductivity was then recalculated. This was done for several different time shifts. The results and the equations used to calculate the correlation coefficient are given below.

Table 5. Time Shift Results

Data Time Shift	Correlation Coefficient, ρ
+3	0.9306
+2	0.9532
+1	0.9716
0	0.9895
-1	0.9795
-2	0.9709
-3	0.9575

$$\rho_{X,Y} = \frac{Cov(X,Y)}{\sigma_X \sigma_Y} \tag{12}$$

$$Cov(X,Y) = E\left[\left(X-\mu_X\right)\left(Y-\mu_Y\right)\right] = \sum_x \sum_y \left(x-\mu_X\right)\left(y-\mu_Y\right) p\left(x,y\right) \tag{13}$$

$$\mu_X = \sum x p_X(x) \tag{14}$$

$$\mu_Y = \sum y p_Y(y) \tag{15}$$

Where: σ_X is the standard deviation of X.

σ_y is the standard deviation of Y.

$p_X(x)$ is the probability that x is a given value within the sample.

$p_y(y)$ is the probability that y is a given value within the sample.

p(x,y) is the probability that x is a certain value given that y is a certain value.

These calculations assume that X and Y, which correspond to temperature and conductivity, are random variables. This means that during an experiment each of these parameters could take on different numerical values, thus making them variable, and the values they take on are randomly drawn from many possible experimental results.

The correlation coefficient is a measure of the degree of linear relationship between two variables. It can have values between -1 and 1. The closer its absolute value is to 1, the greater the linear relationship between the two variables. If the correlation coefficient is positive, as one variable increases, so does the other. Conversely, if it is negative, as one variable increases the other decreases (Devore, 2000).

It can be seen from the time shift results in Table 5 that the correlation coefficient is highest for the zero time shift data, which is highlighted. This means that there is the highest linear relationship between the data as recorded by the REMUS AUV. A time shift in either direction caused degradation in this relationship. So, time shifting the data did not seem to improve its accuracy.

b. CTD Probe Source Voltage Fluctuations

Another possible source of errors was CTD probe source voltage fluctuations. This theory stemmed from the supposition that the vehicle could experience voltage fluctuations during large pitch fin angle change as it transitions from the rising to diving portions of the triangle depth pattern and vice versa. These fluctuations could then potentially affect the performance of the CTD probe.

The REMUS vehicle generates a log of vehicle parameters for each mission. This log file, named state.txt, has records of internal temperature, heading rate, internal pressure, depth, depth goal, optical backscatter, fluorometer reading, voltage, current, ground fault indicator reading, pitch, pitch goal, roll, thruster RPM, thruster RPM goal, compass heading, heading goal, latitude, longitude, dead reckoning latitude, dead reckoning longitude, latitude goal, longitude goal, estimated velocity, heading offset, thruster command, pitch command, rudder command, pitch fin position, rudder fin position, objective number (total and current), percentage of CPU in use, flags, faults, and leg number. In addition to these state parameters, the file also includes several administrative items that do not change during a given mission.

In order to determine the possibility of errors introduced by source voltage fluctuations, vehicle bus voltage and pitch fin angle were plotted. This plot clearly indicated that the vehicle's voltage did not significantly fluctuate during pitch fin angle changes. In fact, its only identifiable trend is a constant decrease in bus voltage, which is expected since the batteries are constantly discharging during the mission. A portion of this plot for distance along the track of approximately 20 km to 22 km is shown below. This region was chosen because there was significant spiking in the raw salinity plot here. So, voltage fluctuations were ruled out as a potential root cause for the anomalies present in the raw data.

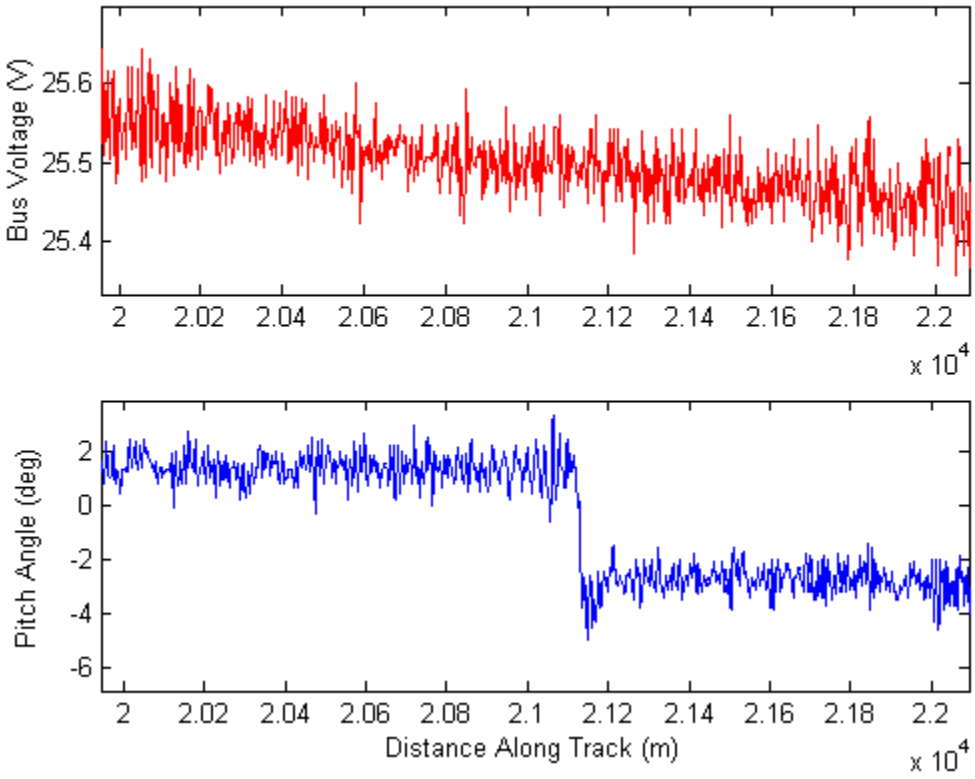

Figure 24. Bus Voltage During Pitch Change

c. Loiter Mission

Another area examined was a comparison of salinity data collected while REMUS was maintaining a constant depth compared to data collected during the triangle depth keeping mode. Unfortunately, it is impossible to have the vehicle collecting data in these two different depth modes from exactly the same location in the ocean at exactly the same time. So, an experiment that would roughly approximate this was performed.

This experiment was designed so that REMUS would attempt to stay at a constant depth while loitering in a given location. Then it would move to another location while changing to a different depth and loiter there. It

would next return to the first location, once again changing depth along the way, and loiter there. This pattern was used to collect data at depths of 3 to 30 meters at 3 meters increments. Then, REMUS would drive through this same area while in triangle depth mode.

In order to allow time for sufficient data to be collected at each given depth increment in the triangle depth mode, several complete diving and rising cycles were needed. So, REMUS had to start approximately 1 km away from the loitering areas and drive approximately 1 km past them during the triangle depth portion of the experiment. Finally, the loitering portion of the experiment was repeated. This was done so that the results of both loitering portions could be averaged to minimize errors due to actual salinity changes over time. The following figures show the vehicle's position during the experiment. The first figure is a close in view of the loitering areas and the second shows the entire experiment.

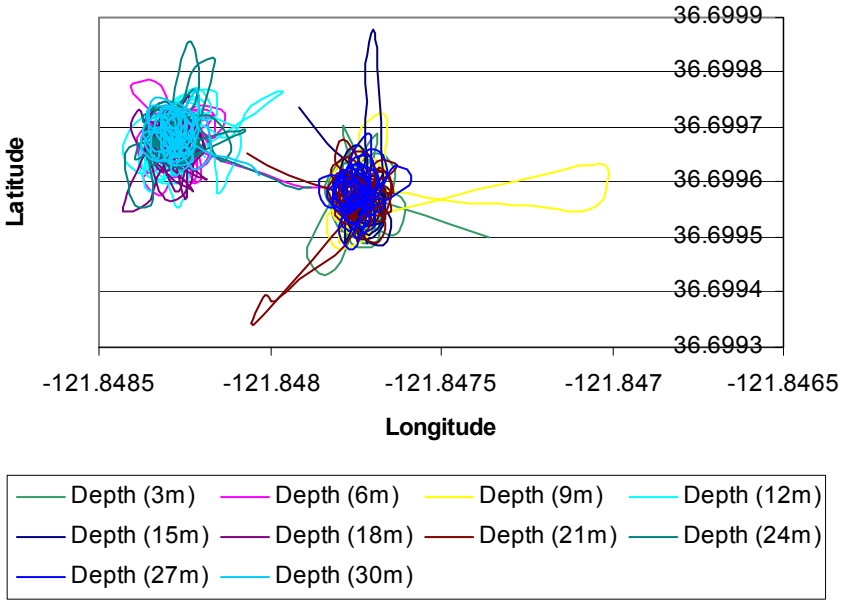

Figure 25. Loiter Positions

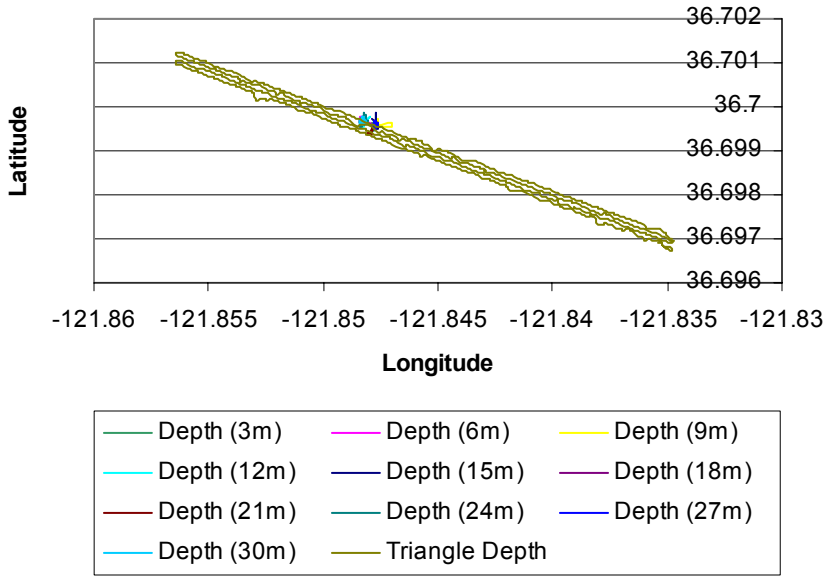

Figure 26. Loiter Experiment Vehicle Position

The vehicle was not able to exactly maintain the desired depths during the loitering portions of the experiment, so the data was filtered such that only those points taken at depths 0.5 meter above and below the desired depth were retained. This was compared to the data taken from the triangle depth portion. In order to facilitate comparison, the triangle depth data was organized into the same depth bins as the loiter data. Some error is introduced by the fact that the data was taken from slightly different locations and at slightly different times.

A plot of the results is shown below. The loiter portion results are the average of the two loitering phases of the experiment. Once again, this was done to minimize errors introduced by the change in salinity over time.

Figure 27. Loiter Mission Results

This plot shows that the salinity values obtained from the triangle depth mode and while loitering at a near constant depth were very close. The largest disparity is only 0.039 ppt at 21 meters of depth. Also, the trends in salinity over depth are very similar.

The data shows in general that the deeper water layers are colder and heavier. This is consistent with a stable ocean. However, in some areas the upper layers were slightly heavier than the middle, indicating unstable layers. Since the differences involved are small it is not clear exactly what to conclude from this. Although it would appear that in this area of Monterey Bay, slight inversion in the very shallow water layer may have been occurring with mixing due to wind and waves.

IV. CONCLUSIONS AND RECOMMENDATIONS

A. CONCLUSIONS

The REMUS AUV has proven itself as a valuable asset for MCM operations in actual field operations. It has also been evaluated many times in controlled field tests, searching for pre-positioned MLOs. It has generally performed well in these tests.

Even so, there is always room for improvement. The experimentation performed in support of this thesis was unlike the other testing. It was designed for a different purpose. The MLO detection results did have comparatively small separations between the means and extreme values of the two different headings. However, the significant result was the apparent course dependency of the data. The fact that detected position of a given MLO could vary by as much as 11.8 meters simply because it was detected on one leg of the area search and not the adjacent one is significant.

REMUS is also routinely used as an oceanographic data collection platform. The Naval Postgraduate School REMUS was tasked with collecting salinity and temperature in Monterey Bay during AOSN II. This data was to be collected over long transects as the vehicle swam a sawtooth pattern between 3 and 50 meters.

REMUS did successfully collect the data but there were inconsistencies with it. There was excessive noise and trends that did not seem possible. When plotted on a mesh plot, there were very jagged boundaries between different density layers and, in some cases, “bubbles” of denser water inside an adjacent layer.

Several potential problems that could cause data inconsistencies were investigated but none seemed to exist. The data was also numerically smoothed. This did improve its appearance but the mesh plots still had the same problems, only to a lesser extent.

A final test was conducted to compare data collected during a sawtooth depth mode with that obtained as the vehicle loitered at almost constant depth. The results from these two modes were very similar. So, it appears that the problems with the data were at least not completely due to the sawtooth depth mode.

B. RECOMMENDATIONS

The mine hunting experiment developed in this thesis needs to be run in other ocean environments and geometries. The amount of disparity between data from the two different legs might change based on the headings of those legs. Also, the effects of current could be substantial. Regardless, this potential course dependence should be investigated further.

Although REMUS is considered to be an AUV well-suited for oceanographic data collection, this is often after having better sensors installed. The installed YSI CTD probe is probably not the best choice for dedicated salinity and temperature collection missions. So, if a REMUS vehicle is to be used for oceanographic missions, it should be fitted with higher resolution sensors.

LIST OF REFERENCES

Allen, B., Stokey, R., Austin, T., Forrester, N., Goldsborough, R., Purcell, M., & von Alt, C. (1997, October). REMUS: A small, low cost AUV; system description, field trials and performance results. *Proceedings of Oceans 1997 MTS/IEEE Conference, 2,* 1132-1136.

von Alt, C. (2003, September). REMUS 100 transportable mine countermeasure package. *Proceedings of Oceans 2003 MTS/IEEE Conference and Exhibition, 3*, 1925-1930.

von Alt, C., Allen, B., Austin, T., Forrester, N., Goldsborough, R., Purcell, M., & Stokey, R. (2001, November). Hunting for mines with REMUS: a high performance, affordable, free swimming underwater robot. *Proceedings of Oceans 2001 MTS/IEEE Conference and Exhibition, 1,* 117-122.

von Alt, C., Allen, B., Austin, T., & Stokey, R. (1994). Remote environmental measuring units. *Proceedings of the Autonomous Underwater Vehicle Conference '94,* 13-19.

American Public Health Association. (1995). *Standard methods for the examination of water and wastewater* (19th ed.). Washington DC: Author.

Clark, V. (2002, October). Seapower 21, projecting force capabilities. *United States Naval Institute Proceedings*,128.

Curtin, T., Bellingham, J., Catipovic, J., & Webb, D. (1993). Autonomous oceanographic sampling networks. *Oceanography,* 6, 86-94.

Devore, J. L. (2000). *Probability and Statistics for Engineering and the Sciences* (5th ed.). Pacific Grove, CA: Brooks/Cole.

Hydroid, Inc. (2003). REMUS 100 operations and maintenance manual. East Falmouth, MA: Author.

Jordan, K. (2003, July/August). Remus AUV plays key role in Iraq war. *Underwater Magazine*, 15-18.

Leonard, J., Bennett, A., Smith, C., & Feder, H. (1998). Autonomous underwater vehicle navigation. *MIT Marine Robotics Laboratory Technical Memorandum,* 98-1.

Marine Sonic Technology, LTD. (1991). Sea Scan® PC operator's manual version 1.6. Gloucester, VA: Author.

Matos, A., Cruz, N., Martins, A. & Periera F. (1999, September). Development and implementation of a low-cost LBL navigation system for an AUV. *Proceedings of Oceans 1999 MTS/IEEE Conference and Exhibition, 2,* 774-779.

Monterey Bay Aquarium Research Institute. (2004, April 30). AOSN. Retrieved May 19, 2004 from the World Wide Web: http://www.mbari.org/aosn/

Purcell, M., von Alt, C., Allen, B., Austin, T., Forrester, N., Goldsborough, R., & Stokey, R. (2000, September). New capabilities of the REMUS autonomous underwater vehicle. *Proceedings of Oceans 2000 MTS/IEEE Conference and Exhibition, 1,* 147-151.

Rennie, J. (2004). Mine warfare vision. 2004 NDIA joint undersea warfare technology spring conference.

Ryan, P. (2003, May). Iraqi Freedom mine countermeasures success. *United States Naval Institute Proceedings, 129*, 52.

Stanton, T. (2003, February). Rapid environmental assessment laboratory (REAL) and Monterey inner shelf laboratory (MISO). Retrieved May 21, 2004 from the World Wide Web: http://www.oc.nps.navy.mil/~stanton/miso/misohome.html

Stokey, R., Austin, T., Allen, B., Forrester, N., Gifford, E., Goldsborough, R., Packard, G., Purcell, M., & von Alt, C. (2001, November). Very shallow water mine countermeasures using the REMUS AUV: a practical approach yielding accurate results. *Proceedings of Oceans 2001 MTS/IEEE Conference and Exhibition, 1,* 149-156.

YSI, Inc. (1999). 6 series environmental monitoring systems. Yellow Springs, OH: Author.

THIS PAGE INTENTIONALLY LEFT BLANK

INITIAL DISTRIBUTION LIST

1. Defense Technical Information Center
   Ft. Belvoir, VA

2. Dudley Knox Library
   Naval Postgraduate School
   Monterey, CA

3. Professor Anthony J. Healey, Code ME/HY
   Department of Mechanical and Astronautical Engineering
   Naval Post Graduate School
   Monterey, CA

4. Dr. T. Swean, Code 32OE
   Office if Naval Research
   Arlington, VA

5. Christopher J. von Alt
   Woods Hole Oceanographic Institution
   Woods Hole, MA

6. Dr. Mark Moline
   Biological Sciences Department
   California Polytechnic State University
   San Luis Obispo, CA

7. Dr. James G. Bellingham
   Monterey Bay Aquarium Research Institute
   Moss Landing, CA